Plate 1
Utah Geological Survey Miscellaneous Publication 173DM
Geologic Map of the Newfoundland Mountains and east part of the Wells 30′ x 60′ Quadrangles

UTAH GEOLOGICAL SURVEY
a division of
Utah Department of Natural Resources
in cooperation with
U.S. Department of the Interior
U.S. Geological Survey

GEOLOGIC MAP OF THE NEWFOUNDLAND MOUNTAINS AND EAST PART OF THE WELLS 30′ X 60′ QUADRANGLES, BOX ELDER COUNTY, UTAH

by
David M. Miller[1], Tracey J. Felger[2], and Victoria E. Langenheim[3]
2021

[1] U.S. Geological Survey, Emeritus, Moffett Field, California
[2] U.S. Geological Survey, Flagstaff, Arizona
[3] U.S. Geological Survey, Moffett Field, California

SCALE 1:62,500

1 0.5 0 1 2 3 4 MILES

1 0.5 0 1 2 3 4 5 6 KILOMETERS

CONTOUR INTERVAL 50 METERS

GREAT SALT LAKE BATHYMETRIC CONTOUR INTERVAL 1 FOOT

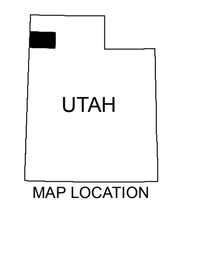

MAP LOCATION

APPROXIMATE MEAN DECLINATION, 2021

This geologic map was funded by the U.S. Geological Survey, National Geologic Mapping Program and the Utah Geological Survey.

Base from USGS Newfoundland Mountains 30′ x 60′ Quadrangle (1988)
and USGS Wells 30′ x 60′ Quadrangle (1981)
Shaded relief derived from USGS 10-meter NED
Projection: UTM Zone 12
Datum: NAD 1927
Spheroid: Clarke 1866

Project Manager: Donald L. Clark
GIS and Cartography: Tracey J. Felger (USGS) and Rosemary I. Fasselin (UGS)

Utah Geological Survey
1594 West North Temple, Suite 3110
Salt Lake City, UT 84116
(801) 537-3300
https://geology.utah.gov
https://doi.org/10.34191/MP-173DM

UTAH GEOLOGICAL SURVEY
a division of
Utah Department of Natural Resources
in cooperation with
U.S. Department of the Interior
U.S. Geological Survey

CORRELATION OF MAP UNITS

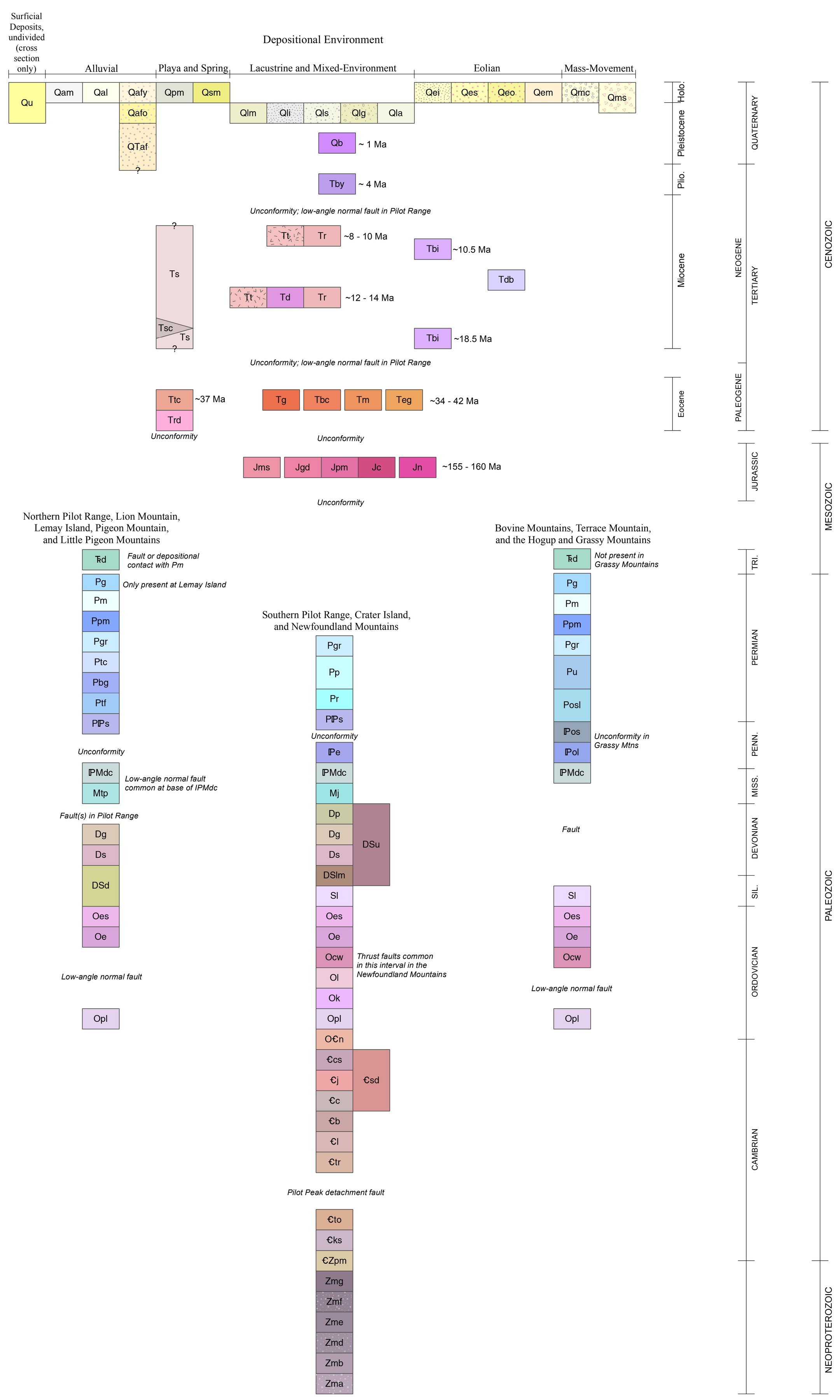

LIST OF MAP UNITS

Quaternary-Tertiary Surficial Deposits

- Qu — Surficial deposits, undivided (Holocene and Pleistocene)

Alluvial Deposits

- Qam — Alluvial mud (Holocene)
- Qal — Stream alluvium (Holocene)
- Qafy — Young alluvial-fan deposits (Holocene)
- Qafo — Older alluvial-fan deposits (Pleistocene)
- QTaf — Oldest alluvial-fan deposits (Pleistocene and Pliocene?)

Playa and Spring Deposits

- Qpm — Playa mud (Holocene)
- Qsm — Spring mud (Holocene)

Lacustrine and Mixed-Environment Deposits

- Qlm — Lacustrine marl (Pleistocene)
- Qli — Lacustrine silt (Pleistocene)
- Qls — Lacustrine sand (Pleistocene)
- Qlg — Lacustrine gravel (Pleistocene)
- Qla — Lacustrine and alluvial deposits, undivided (Pleistocene)

Eolian Deposits

- Qei — Eolian silt (Holocene)
- Qes — Eolian sand and silt (Holocene)
- Qeo — Eolian ooid sand (Holocene)
- Qem — Eolian mud (Holocene)

Mass-Movement Deposits

- Qmc — Colluvium and talus (Holocene)
- Qms — Landslide deposits (Holocene and Pleistocene)

Quaternary Volcanic Rocks

- Qb — Basalt of Sheep Mountain (Pleistocene)

Tertiary (Neogene) Igneous and Sedimentary Rocks

- Tby — Younger basaltic lava flows (Pliocene)
- Ts — Salt Lake Formation, undivided (Miocene)
- Tsc — Salt Lake Formation, conglomerate (Miocene)
- Tt — Tuff and tuff breccia (Miocene)
- Tr — Rhyolite (Miocene)
- Td — Dacite (Miocene)
- Tbi — Intermediate-age basaltic lava flows (Miocene)
- Tdb — Diabase (Miocene)

Tertiary (Paleogene) Igneous and Sedimentary Rocks

- Ttc — Rhyolitic tuff and sedimentary rocks (Eocene)
- Trd — Rhyodacite (Eocene)
- Tg — Granodiorite dikes (Eocene)
- Tbc — Bettridge Creek Granodiorite (Eocene)
- Tm — McGinty Monzogranite (Eocene)
- Teg — Emigrant Pass intrusion of Compton and others (1977) (Eocene)

Jurassic Plutonic Rocks

- Jms — Miners Spring Granite
- Jgd — Granodiorite
- Jpm — Porphyritic monzogranite
- Jc — Crater Island Quartz Monzonite
- Jn — Newfoundland Stock of Caroon (1977)

Triassic Rocks

- ₮d — Dinwoody Formation

Permian Rocks

- Pg — Gerster Formation
- Pm — Murdock Mountain Formation
- Ppm — Phosphoria Formation, Meade Peak Phosphatic Shale Tongue
- Pgr — Grandeur Formation of the Park City Group
- Ptc — Trapper Creek Formation
- Pbg — Badger Gulch Formation
- Pp — Pequop Formation
- Pu — Unnamed sandstone unit
- Ptf — Third Fork(?) Formation
- Pr — Riepetown Sandstone

Permian and Pennsylvanian Rocks

- Posl — Oquirrh Group, Interbedded sandstone and limestone unit
- ℙos — Oquirrh Group, Sandstone unit
- ℙol — Oquirrh Group, Limestone unit
- Pℙs — Strathearn Formation
- ℙe — Ely Limestone

Pennsylvanian and Mississippian Rocks

- ℙMdc — Diamond Peak Formation and Chainman Shale, undivided

Mississippian Rocks

- Mtp — Tripon Pass Limestone
- Mj — Joana Limestone

Devonian Rocks

- Dp — Pilot Shale
- Dg — Guilmette Formation
- Ds — Simonson Dolomite

Devonian and Silurian Rocks

- DSd — Thick–bedded dolomite, undivided
- DSlm — Lone Mountain Dolomite
- DSu — Undivided dolomite and limestone

Silurian Rocks

- Sl — Laketown Dolomite

Ordovician Rocks

- Oes — Ely Springs Dolomite
- Oe — Eureka Quartzite
- Ocw — Crystal Peak Dolomite and Watson Ranch Quartzite
- Ol — Lehman Formation
- Ok — Kanosh Shale
- Opl — Lower Pogonip Group

Ordovician and Cambrian Rocks

- O€n — Notch Peak Formation

Cambrian Rocks

- €cs — Corset Spring Shale Member of the Orr Formation
- €j — Johns Wash Limestone Member of the Orr Formation
- €c — Candland Shale Member of the Orr Formation
- €sd — Sandstone and dolomite
- €b — Big Horse Limestone Member of the Orr Formation
- €l — Lamb Dolomite
- €tr — Trippe Limestone
- €to — Toano Limestone
- €ks — Killian Springs Formation

Cambrian and Neoproterozoic Rocks

- €Zpm — Prospect Mountain Quartzite

Neoproterozoic Rocks

- Zmg — McCoy Creek Group of Misch and Hazzard (1962), Unit G
- Zmf — McCoy Creek Group of Misch and Hazzard (1962), Unit F
- Zme — McCoy Creek Group of Misch and Hazzard (1962), Unit E
- Zmd — McCoy Creek Group of Misch and Hazzard (1962), Unit D
- Zmb — McCoy Creek Group of Misch and Hazzard (1962), Unit B(?)
- Zma — McCoy Creek Group of Misch and Hazzard (1962), Unit A(?)

GEOLOGIC SYMBOLS

- Contact – Long dashed where approximately located, short dashed where inferred, dotted where concealed
- Bedding plane fault – Long dashed where approximately located, dotted where concealed; ticks on hanging wall
- Overturned low-angle normal fault – Dotted where concealed; teeth on hanging wall
- Low-angle normal fault – Long dashed where approximately located, dotted where concealed; teeth on hanging wall
- Steeply dipping normal fault – Long dashed where approximately located, short dashed where inferred, dotted where concealed; bar and ball on downthrown side
- Normal fault, geophysical, gravity – Dotted where concealed and very approximately located; bar and ball on downthrown side
- Thrust fault – Dotted where concealed; teeth on hanging wall
- Fault, unknown type – Long dashed where approximately located, dotted where concealed
- Fault, gravity slide – Ticks on hanging wall
- Zone of structural accommodation

Lake Bonneville shorelines --

- Bonneville shoreline – Dashed where approximately located
- Provo shoreline – Dashed where approximately located
- Stansbury shoreline
- Pilot Valley shoreline – Dashed where approximately located
- Gilbert shoreline – Dashed where approximately located

- Axial trace of anticline – Dotted where concealed
- Axial trace of syncline – Dotted where concealed
- Line of cross section
- Bedding form lines (cross section only)

Sedimentary bedding attitude -

- Inclined
- Inclined, orientation approximate
- Overturned
- Vertical

Volcanic and metamorphic foliation -

- Horizontal
- Inclined
- Vertical

- Ground water well
- Drill hole – Oil/gas exploration

INDEX TO GEOLOGIC MAPPING

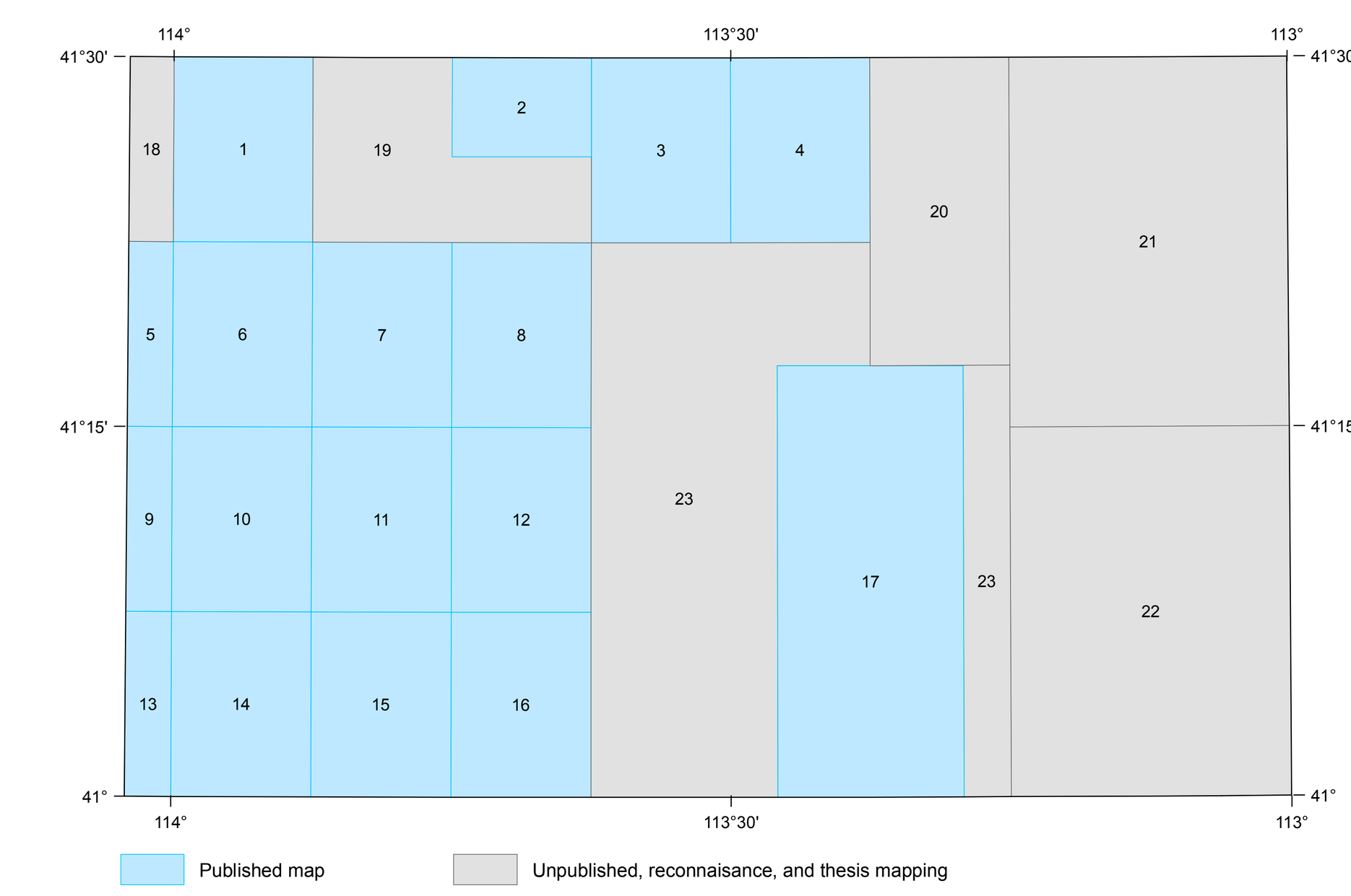

MAP NAME AND AUTHORS

1. Lucin NW - Miller and Oviatt, 1994
2. Bovine Mountain - Jordan, 1983
3. Terrace Mountain West - Miller and McCarthy, 2002
4. Terrace Mountain East - McCarthy and Miller, 2002
5. Tecoma - Miller and Schneyer, 1985
6. Lucin - Miller, 1985
7. Pigeon Mountain - Glick and Miller, 1987
8. Jackson - Miller and Glick, 1987
9. Patterson Pass - Miller and others, 1993
10. Crater Island NW - Miller, 1993
11. Lemay Island - Miller and Glick, 1986
12. Lucin 4 NW - Glick and Miller, 1986
13. Pilot Peak - Miller and Lush, 1994
14. Crater Island SW - Miller, 1990c
15. Crater Island - Miller and others, 1990a
16. Lucin 4 SW - Miller, 1990a
17. Newfoundland Mountains - Allmendinger and Jordan, 1989
18. Jackson Spring area - Douglas, 1984; Miller and Felger, unpublished mapping
19. Lucin NE-Bovine area - Miller and Felger, unpublished mapping; Compton and others, 1983, unpublished mapping
20. Sheep Mountain area - Miller and Felger, unpublished mapping
21. Hogup Mountains area - Stifel, 1964; Miller, unpublished mapping
22. Grassy Mountains area - Doelling, 1964; Miller, unpublished mapping
23. Great Salt Lake Desert - Miller, unpublished mapping

LITHOLOGIC COLUMN

Cenozoic Rocks

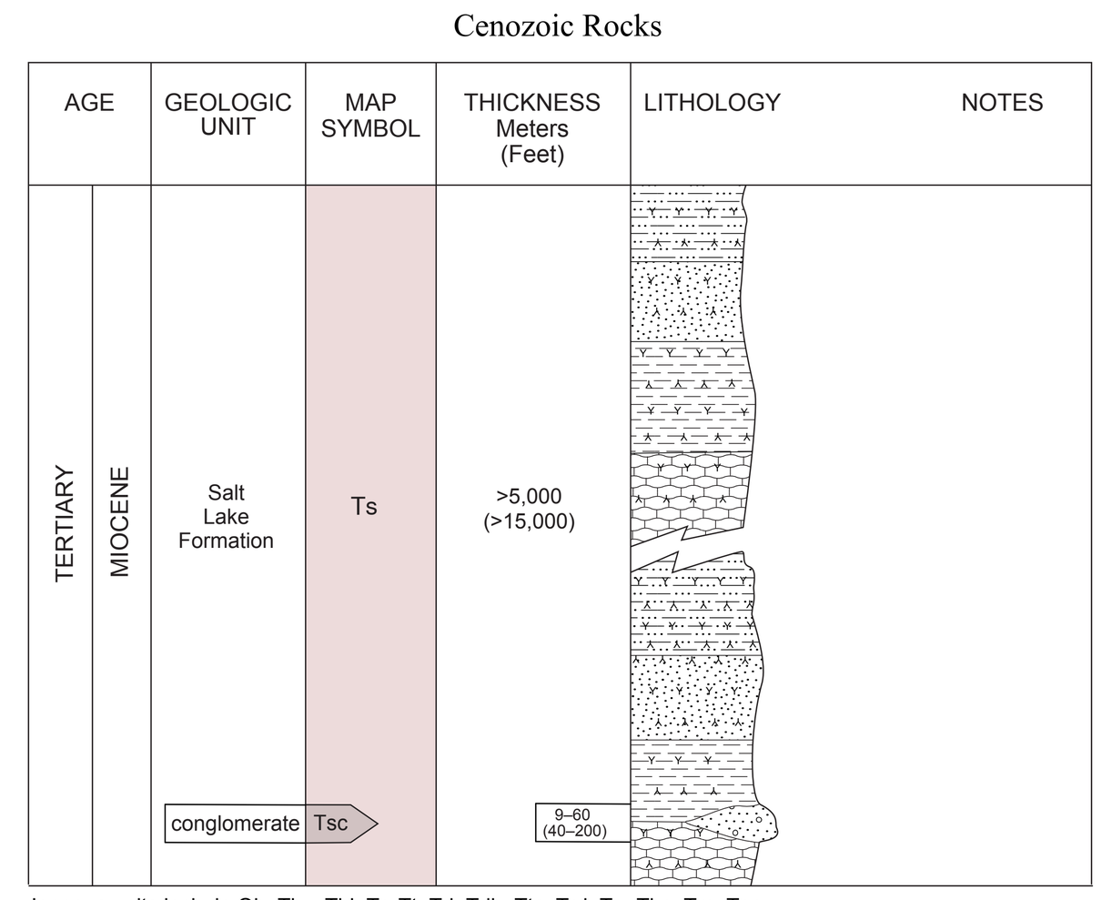

Igneous units include Qb, Tby, Tbi, Tr, Tt, Td, Tdb, Ttc, Trd, Tg, Tbc, Tm, Teg

LITHOLOGIC COLUMN

Northern Pilot Range, Lion Mountain, Lemay Island, Pigeon Mountain, and Little Pigeon Mountains

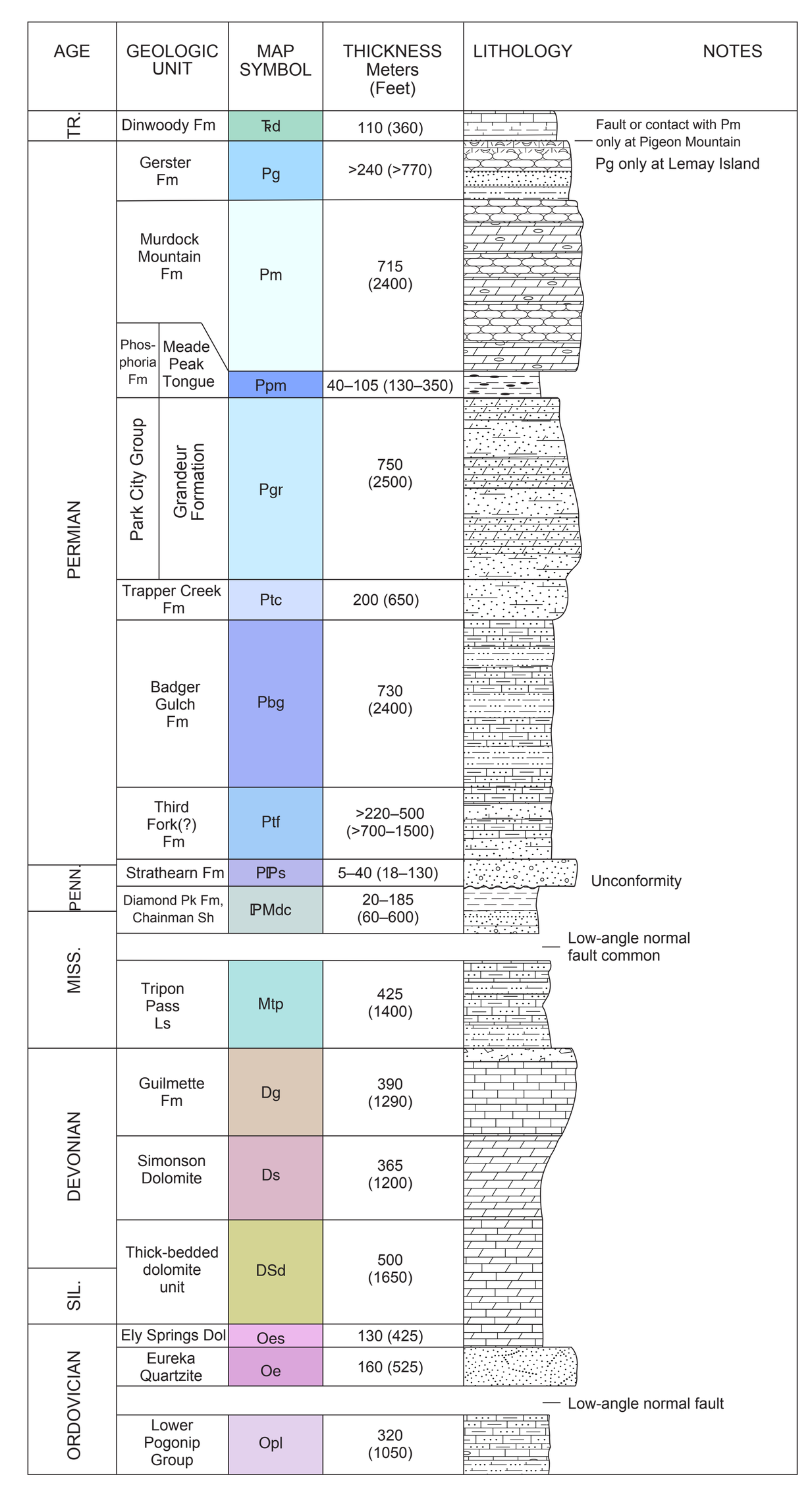

LITHOLOGIC COLUMN

Southern Pilot Range, Crater Island, Newfoundland Mountains

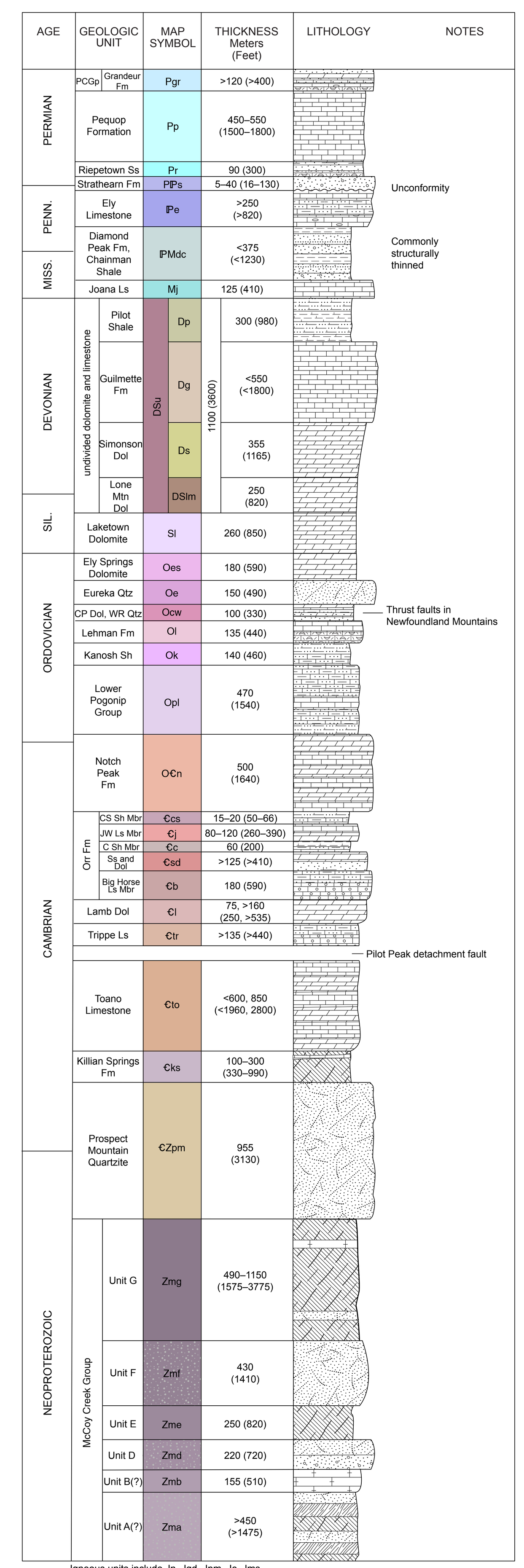

Igneous units include Jn, Jgd, Jpm, Jc, Jms

LITHOLOGIC COLUMN

Bovine Mountains, Terrace Mountain, Hogup Mountains, Grassy Mountains

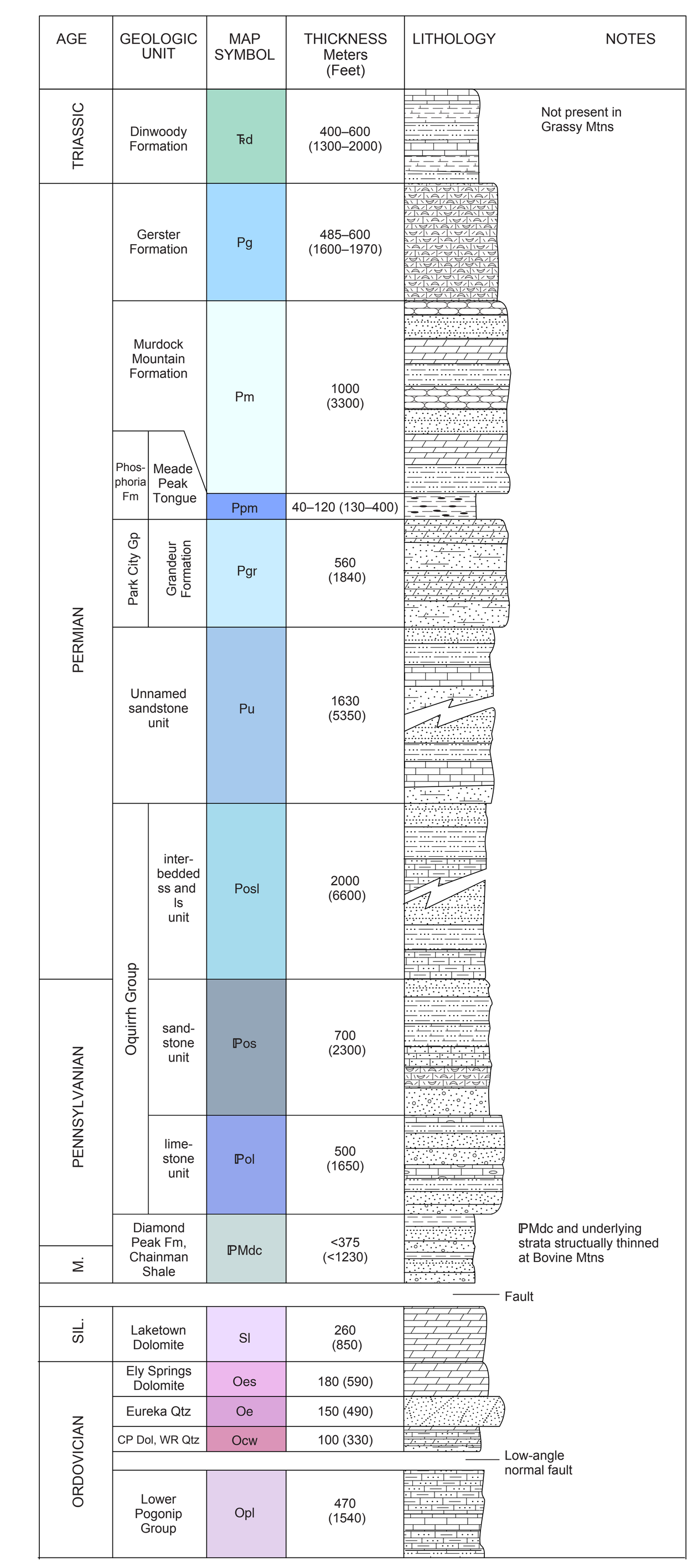

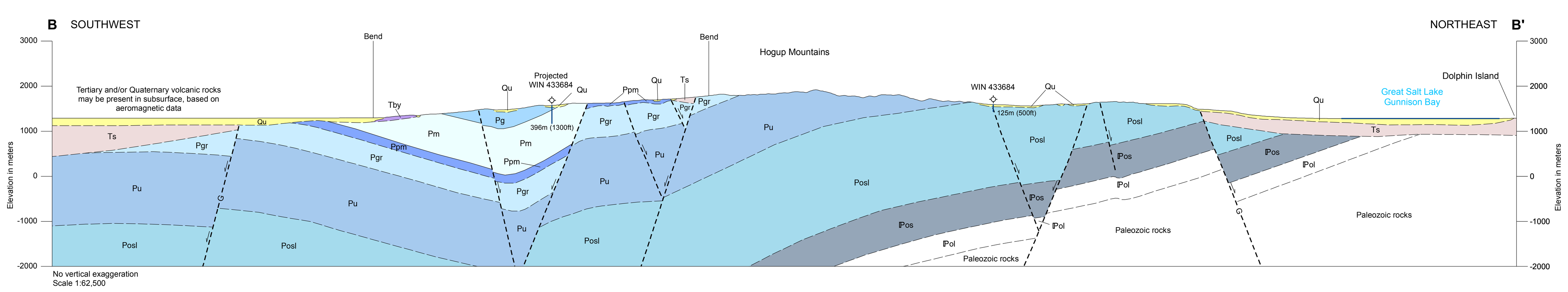

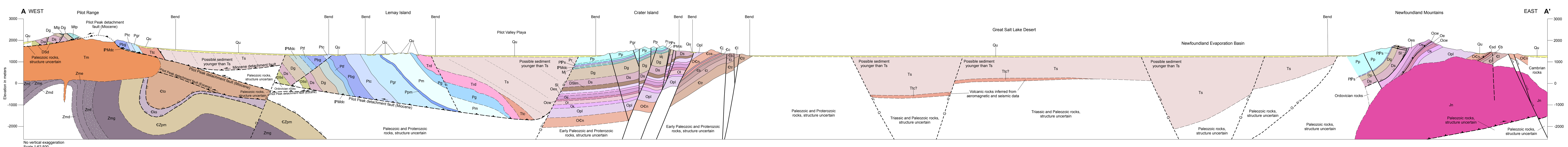

GEOLOGIC AND GEOPHYSICAL MAPS OF THE NEWFOUNDLAND MOUNTAINS AND PART OF THE ADJACENT WELLS 30' X 60' QUADRANGLES, BOX ELDER COUNTY, UTAH

by David M. Miller, Tracey J. Felger, and Victoria E. Langenheim

MISCELLANEOUS PUBLICATION 173DM
UTAH GEOLOGICAL SURVEY
UTAH DEPARTMENT OF NATURAL RESOURCES
in cooperation with
U.S. GEOLOGICAL SURVEY
U.S. DEPARTMENT OF THE INTERIOR
2021

Blank pages are intentional for printing purposes.

GEOLOGIC AND GEOPHYSICAL MAPS OF THE NEWFOUNDLAND MOUNTAINS AND PART OF THE ADJACENT WELLS 30' X 60' QUADRANGLES, BOX ELDER COUNTY, UTAH

by David M. Miller [1], Tracey J. Felger [2], and Victoria E. Langenheim [3]

[1] U.S. Geological Survey, Emeritus, Moffett Field, California
[2] U.S. Geological Survey, Flagstaff, Arizona
[3] U.S. Geological Survey, Moffett Field, California

Cover photo: *View south from Desert Peak of the Newfoundland Mountains showing adjacent mud flats (playas) of the Great Salt Lake Desert. Light-colored rocks in the foreground are Ordovician Eureka Quartzite and brownish-gray rocks to the south are Permian through Ordovician strata. Photo by Adam Hiscock.*

Suggested citation:

Miller, D.M., Felger, T.J, and Langenheim V.E., 2021, Geologic and geophysical maps of the Newfoundland Mountains and part of the adjacent Wells 30' x 60' quadrangles, Box Elder County, Utah: Utah Geological Survey Miscellaneous Publication 173DM, 26 p., 2 plates, scale 1:62,500, https://doi.org/10.34191/MP-173DM.

MISCELLANEOUS PUBLICATION 173DM
UTAH GEOLOGICAL SURVEY
UTAH DEPARTMENT OF NATURAL RESOURCES
in cooperation with
U.S. GEOLOGICAL SURVEY
U.S. DEPARTMENT OF THE INTERIOR
2021

STATE OF UTAH
Spencer J. Cox, Governor

DEPARTMENT OF NATURAL RESOURCES
Brian Steed, Executive Director

UTAH GEOLOGICAL SURVEY
R. William Keach II, Director

PUBLICATIONS
contact
Natural Resources Map & Bookstore
1594 W. North Temple
Salt Lake City, UT 84116
telephone: 801-537-3320
toll-free: 1-888-UTAH MAP
website: utahmapstore.com
email: geostore@utah.gov

UTAH GEOLOGICAL SURVEY
contact
1594 W. North Temple, Suite 3110
Salt Lake City, UT 84116
telephone: 801-537-3300
website: geology.utah.gov

This geologic map was funded by the U.S. Geological Survey, National Geologic Mapping Program and the Utah Geological Survey.

CONTENTS

FIGURES

TABLES

PLATES

GEOLOGIC AND GEOPHYSICAL MAPS OF THE NEWFOUNDLAND MOUNTAINS AND PART OF THE ADJACENT WELLS 30' X 60' QUADRANGLES, BOX ELDER COUNTY, UTAH

by David M. Miller, Tracey J. Felger, and Victoria E. Langenheim

INTRODUCTION

The Newfoundland Mountains map area (Newfoundland Mountains and adjacent part of Wells 30' x 60' quadrangles) is located in Box Elder County, northwestern Utah. The map encompasses broad expanses of the Great Salt Lake Desert as well as several picturesque mountain ranges (figures 1, 2, and 3). The geology of the area was last mapped and summarized by Doelling (1980). Since that landmark study, much of the area has been mapped in greater detail and new paleontologic, geochronologic, and structural data provide for an updated view of the geology. In addition, new geophysical studies (Langenheim and others, 2013; Langenheim, 2016) provide key data for improved interpretation of subsurface geology.

The geologic map (plate 1) was compiled from fifteen 7.5' quadrangles mapped at a scale of 1:24,000 (mostly in the western part of the area), one map covering the Newfoundland Mountains at a scale of 1:31,680 (Allmendinger and Jordan, 1989), unpublished geologic mapping at scales from 1:24,000 to 1:50,000 (most by Miller; Bovine Mountain by T.E. Jordan), and reconnaissance mapping and aerial photo interpretation in intervening areas by Miller. Some published maps were remapped or reinterpreted by the authors in light of more recent studies north of the map area. Geologic mapping conducted as part of several theses/dissertations and a few published papers also were used (plate 2, index to geologic mapping). Concealed faults under valley bottoms were interpreted from gravity and aeromagnetic data.

Our approach for this map was to integrate across the main themes of the mapped geology by generalizing units, structures, and polygons. This has the aim of illustrating the principal tectonic and stratigraphic packages, as well as illustrating the patterns of surficial units and geomorphology. Cross sections (plate 2) were constructed to coincide with representative cross sections for several detailed geologic maps. This approach required large bends across valleys. Basin geometry shown in the cross sections was constrained by gravity data and a seismic line since few deep drill holes are available.

OVERVIEW OF THE GEOLOGY

The Newfoundland Mountains map area is located within the Basin and Range Province, and exhibits many fault-bounded mountains separated by broad valleys (figure 1). Neoproterozoic to Pliocene rocks crop out in the mountains. Basins are mainly mantled by alluvial fans and playas that are covered in some places by extensive thin deposits from Lake Bonneville.

Rocks as old as Neoproterozoic are present in the Pilot Range (figure 3) where they are metamorphosed to various degrees (Miller and others, 1987; Miller and Hoisch, 1995). These rocks, along with overlying metamorphosed Cambrian formations, are structurally overlain by diverse Paleozoic and Mesozoic strata that lie above the Pilot Peak detachment fault, which was active during both the Eocene and Miocene. Paleozoic and sparse early Mesozoic sedimentary rocks differ in thickness and lithologic character from east to west as well as north to south (Miller and others, 1991) as a result of rapid facies changes and juxtaposition by structures during the Mesozoic and Cenozoic. We combine rock units into groups for this map. Two sequences of Pennsylvanian and Permian units are distinguished by presence or absence of the Oquirrh Group, above which Permian strata are also distinct. The Oquirrh-bearing sequence lies in the eastern and northern part of the map area. The sequence that does not have the Oquirrh generally exhibits a profound unconformity, above which the Strathearn Formation, a conglomerate, occurs. Significant lateral changes occur in the Permian units above the Strathearn so the sections in the north were split from those in the south.

Mesozoic tectonics consisted of both thrusting and extension before or during Jurassic intrusion of plutons (Allmendinger and Jordan, 1984; Miller and others, 1987; Miller and Allmendinger, 1991). Subsequent thrust faults that surfaced far to the east underlie the exposed rocks of the quadrangle; the exposed rocks were passively rafted eastward during the Cretaceous and early Paleogene (Allmendinger and Jordan, 1984). One of these deeper thrust faults, a concealed thrust fault that separates rocks of the Newfoundland Mountains and the Grassy Mountains to the east, is inferred on the basis of dramatic facies change in upper Paleozoic rocks (Allmendinger and Jordan, 1984).

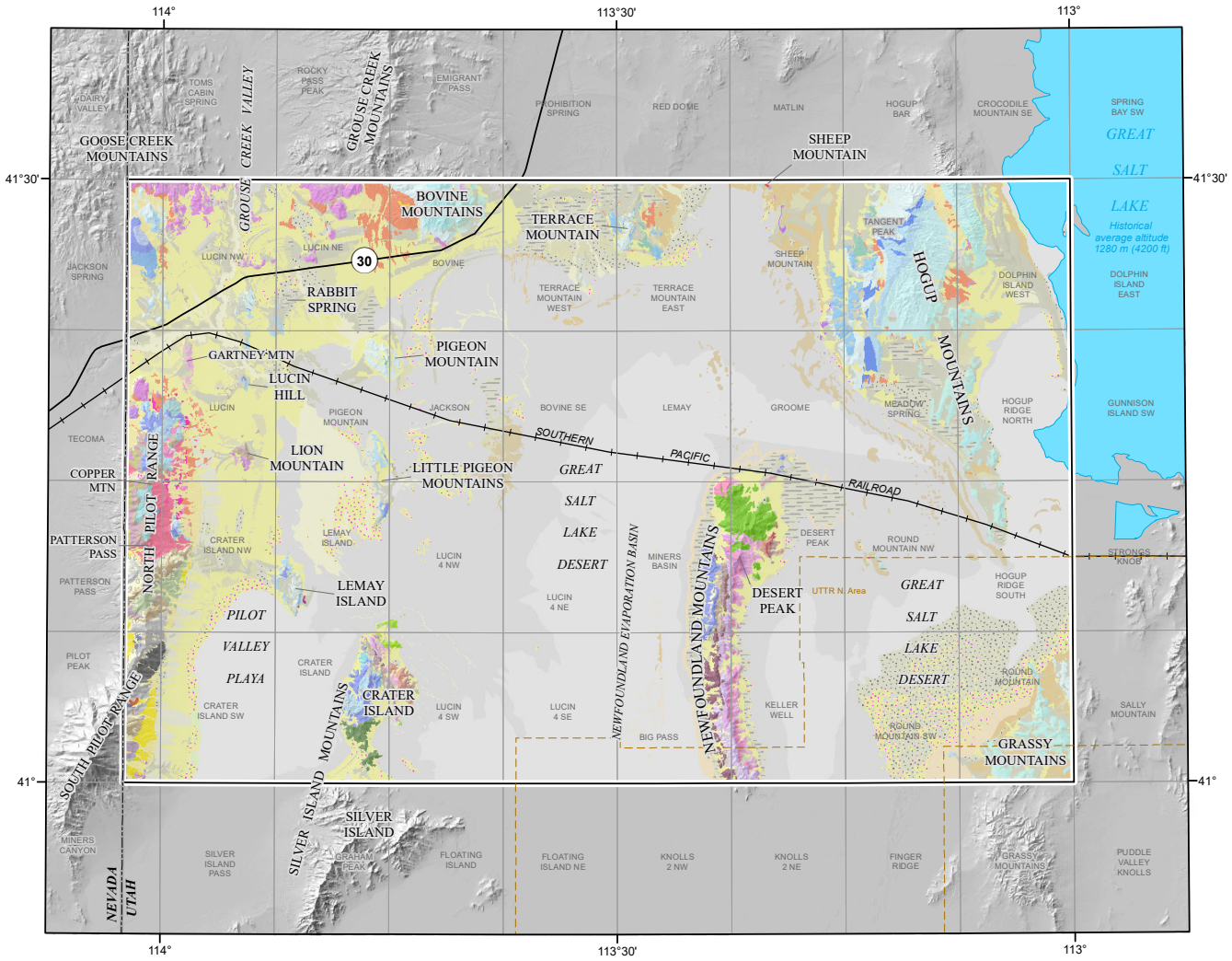

Figure 1. *Main features and geology in Newfoundland Mountains map area and a bordering area of Utah and Nevada. UTTR is Utah Test and Training Range (U.S. Air Force). Gray lines and text are 7.5' quadrangle boundaries and names.*

Figure 2. *View southeast from Grouse Creek Mountains of the Great Salt Lake Desert with the Newfoundland Mountains beyond. The low ridge in the foreground with light sediment in front is a barrier beach deposited during the highstand of Lake Bonneville. The salt flats conceal a complex bedrock surface as inferred from gravity data. Photo by T.J. Felger.*

Figure 3. *Pilot Peak and a damp Pilot Valley playa in the foreground. Forested slopes are primarily underlain by the Prospect Mountain Quartzite and overlying metamorphic rocks. Foothills are underlain by down-faulted rocks and modified by Lake Bonneville shorelines. View to the northwest from Silver Island Mountains. Photo by T.J. Felger.*

Cenozoic tectonics consisted of two extensional events—one in the Eocene and one in the Miocene, each with associated volcanism and sedimentary basin filling. Small late Eocene granodiorite plutons and compositionally similar volcanic rocks are common in the Pilot Range. Some Eocene intrusions cut deformed rocks in the Pilot Peak detachment and are in turn cut by faults in the Pilot Peak detachment, indicating that in the southern Pilot Range the Pilot Peak detachment is a composite detachment fault that had deep-seated faulting during the Eocene or earlier, followed by extension after the Eocene (Miller, 1990b). In the central Pilot Range, the Eocene McGinty pluton (unit Tm) occupies a major structural break that places non-metamorphosed Ordovician rocks on metamorphosed Early Cambrian rocks and thus apparently intruded the Eocene Pilot Peak detachment. The top of the pluton was subsequently sliced off by the Miocene Pilot Peak detachment that warps over the range and carries rocks as young as middle Miocene in its hanging wall. Both faults carry steeply east-tilted Paleozoic and Tertiary strata on their hanging walls that require offset along the fault to be top-to-the-west; they are illustrated in cross section A-A' (plate 2). The eastern breakaway for the faults is inferred to lie between dissimilar Paleozoic strata on Lemay Island and Crater Island. Although some hallmarks of metamorphic core complexes are exhibited by the Pilot Range (major detachment faults, metamorphism of lower plate rocks), evidence for detachment faults that rooted in the ductile realm, such as mylonitic rocks that are overprinted by breccia, are lacking. We consider the area to be a strongly extended terrane.

Eocene plutons and volcanic rocks dated by K-Ar commonly yielded ages that are close to the Oligocene-Eocene boundary. These rocks are compositionally similar and were interpreted as Eocene in age by Miller and others (1987) because a U-Pb age for one pluton is ~39 Ma. Miocene volcanic rocks in many places lie within or on poorly dated sedimentary sequences that contain abundant reworked volcanic ash. Both bimodal volcanism and thick sedimentary sequences are characteristic of late Cenozoic Basin and Range extensional tectonics (e.g., Best and others, 1989; Miller, 1990b). The ash-rich Salt Lake Formation (unit Ts) is the primary example of late Cenozoic extensional basin deposits in this region (figure 4). It locally consists of lacustrine facies and is interbedded with basalt to rhyolite lava flows in a few areas. A volcanic field studied by Fiesinger and others (1982) in the northwest corner of the map area interfingers with and overlies the upper part of the Salt Lake Formation (figures 5 and 6). The field is composed of rhyolite and dacite lava flows and domes that are about 14 to 8 Ma (Miller and Oviatt, 1994), and represent the youngest extensive volcanism during the Miocene in the Newfoundland Mountains map area. Pliocene to Quaternary

Figure 4. *Gently dipping thin beds of shale, siltstone, and ash in the Salt Lake Formation south of Bovine Mountain. Newfoundland Mountains in the background. View is to the southeast. Photo by T.J. Felger.*

Figure 5. *Isolated hills underlain by rhyolite lava domes south of Grouse Creek Mountains. The Bonneville shoreline forms a well-developed wave-cut notch in the dome on the right side of the photo. A barrier beach that formed between the Bonneville and Provo levels extends to the left of the dome, and a white playa trapped upslope of the beach occupies the former lagoon. In the distance are the Great Salt Lake Desert and the Newfoundland Mountains. View is to the southeast. Photo by T.J. Felger.*

Figure 6. *Boldly prominent domes of rhyolite in the northwest corner of the Newfoundland Mountains quadrangle. Domes are 12 to 8 Ma. Prominent dark bands are glassy chilled bases of flows within the domes. View to the north. Photo by T.J. Felger.*

basalt flows are present in the northeastern part of the map area and are part of a much larger concealed volcanic field as indicated by aeromagnetic data (indicated on cross section B-B') (Langenheim, 2016).

Lacustrine and alluvial-fan deposits are the most common Quaternary materials in the map area. Pleistocene alluvial fans were eroded and overlapped by lacustrine sediments deposited during the rise of Lake Bonneville, the youngest and deepest of several large pluvial lakes that formed in northern Utah (Oviatt and others, 1992; Oviatt, 2015). Plate 1 shows mapped intervals of the major shorelines, which are described below. Many more shorelines have been mapped and are present in the GIS database that accompanies this report but not displayed on plate 1 to preserve clarity. The additional shorelines formed in both the transgressive and regressive lake. The earliest recognized shoreline of Lake Bonneville in both the Newfoundland Mountains map area and the greater Lake Bonneville basin is the Pilot Valley shoreline. This shoreline, which was named for distinctive gravel beaches that formed on the eastern, northern, and western sides of Pilot Valley playa (figure 1; Miller and Phelps, 2016), is characterized by one to three beach crests that occur between about 1305 and 1312 meters (4281 and 4304 ft) elevation (figure 7). The Pilot Valley shoreline is commonly misidentified as the Gilbert shoreline; however, it is 7 to 10 meters (23–33 ft) higher in elevation than the Gilbert shoreline (figure 7), and it exhibits transgressive-phase stratigraphy, with marl overlying beach gravel. The Pilot Valley shoreline is poorly dated at about 30 ka. Lake Bonneville rose rapidly across the basin from about 30 ka to 19 ka (all radiocarbon ages are calibrated to Intcal13; Reimer and others, 2013). The intervening Stansbury oscillation, which occurred at about 25 ka, (Oviatt, 2015), produced a series of tufa-cemented gravel and barrier beaches that were deposited throughout the basin (Oviatt and others, 1990). Within the map area, this interval is represented by a complex array of gravel bars and abrasion notches (some with well-developed tufa) between 1363 and 1377 meters (4472 and 4517 ft) elevation (figure 7).

Lake Bonneville reached its maximum depth at about 18.2 ka (Oviatt and others, 1992; Miller and others, 2013) when it formed the Bonneville shoreline. This shoreline forms a conspicuous abrasion notch or platform in the mountain ranges (figure 5) within the map area at elevations between 1579 and 1620 meters (5180–5315 ft) above sea level (figure 7), with the lowest elevations occurring in the Lucin area (figure 1) and the highest elevations occurring in the Newfoundland and Grassy Mountains. Shortly after reaching its maximum depth, the lake overflowed its alluvial threshold in southern Idaho, causing it to catastrophically fail (Bonneville Flood). The flood lowered the lake more than 100 meters (330 ft) to a stable threshold that was occupied from about 18 to 15 ka (Godsey and others, 2005; Miller and others, 2013), forming the Provo shoreline. This shoreline occurs within the map area between elevations of about 1467 and 1497 meters (4813–4911 ft) (figure 7), and is commonly marked by well-developed tufa, especially in areas underlain by bedrock. Like the Bonneville shoreline, the low-

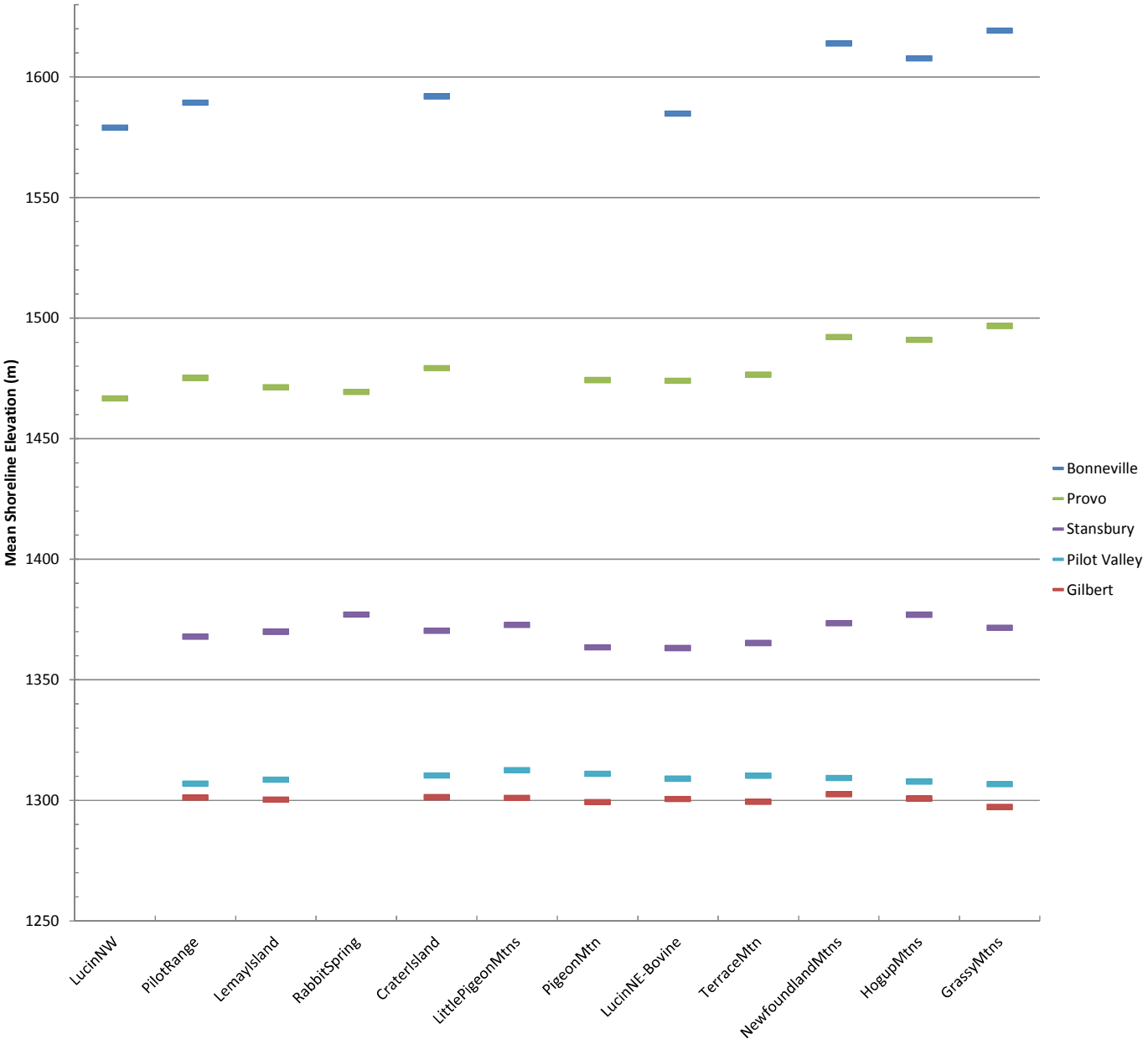

Figure 7. *Mean elevations of regionally correlative Lake Bonneville shorelines across the Newfoundland Mountains map area. Shorelines were grouped into twelve geographic areas (figure 1), and the mean elevation value for each shoreline in each area was derived from 5-meter Digital Elevation Model (DEM) data (https://gis.utah.gov/data/elevation-and-terrain/). Shorelines without a corresponding tic in a given geographic area are not present in that area, in most cases because the topography was too high or too low to preserve the shoreline.*

est elevations of the Provo shoreline are in the Lucin area (figure 1), and the highest elevations are in the Newfoundland and Grassy Mountains. These mountain ranges are situated in what was the deepest part of the Lake Bonneville basin, and thus document the effects of the isostatic rebound that occurred after the lake load was removed (Crittenden, 1963; Chen and Maloof, 2017). Isostatic rebound strongly deformed the Bonneville and Provo shorelines, which show 40 meters and 30 meters (131 and 98 ft) of elevation change, respectively, across the map area (figure 7). In contrast, the elevations of both the Pilot Valley and Gilbert shorelines only vary by about 5 meters (16 ft) across the map area, indicating negligible effects of rebound. In addition to the variability in shoreline elevations that is attributed to isostatic rebound, shoreline features at the Bonneville and Provo levels in the Newfoundland map area commonly show as much as 8 meters (26 ft) of variability along lengths of 500 to 1000 meters (1640–3280 ft). Some of this variation could be due to modification of the shoreline by surficial processes, which makes it difficult to consistently map the same part of a feature for its entire length; however, it also could be reflecting the effects of primary lacustrine processes such as wave energy, or tectonic effects. After 15 ka the lake level fell to very low elevations.

A subsequent rise of early Great Salt Lake took place about 12 to 11.5 ka (Oviatt and others, 2005), and formed the Gil-

bert shoreline, which has elevations within the map area of about 1297 to 1302 meters (4255–4272 ft) above sea level (figure 7). This lake activity left most lowlands blanketed by marl, mud, sand, and gravel. Subsequent erosion and alluvial deposition has modified the landscape only slightly, except along the flanks of the Pilot Range, where alluvial-fan deposition has been robust. Widespread mud flats in the Great Salt Lake Desert are underlain by Lake Bonneville marl, thin alluvial muds associated with numerous small streams, and playa deposits associated with ephemeral lakes.

OVERVIEW OF THE GEOPHYSICS

Gravity and magnetic data are useful for projecting the surface geology into the subsurface. Gravity data are processed to reflect density variations within the upper and middle crust ("isostatic gravity anomaly") and are particularly well suited for determining the shape of Cenozoic basins because of the significant density contrast between dense basement (here defined to be pre-Cenozoic in age) and less dense Cenozoic rocks and deposits. Magnetic data reflect magnetization variations within the crust and are well suited for mapping the distribution of rock types that contain magnetite, such as mafic igneous rocks. Both gravity and magnetic anomalies can be related to rock type, providing a means to map remotely some aspects of the geology. Gravity and magnetic data can also be used to model the location and geometry of faults that juxtapose rocks of differing density and magnetic properties, in particular, those faults responsible for uplifting the Pilot Range and Newfoundland Mountains and for forming basins in the hanging walls of the detachment and normal faults.

The gravity map was created from measurements compiled from several sources, as detailed in Langenheim and others (2013). The data were processed using standard formulas to determine isostatic residual gravity values, which should reflect lateral density variations within the mid- to upper crust. This map (figure 8) represents an improvement upon the Bouguer gravity maps of Cook and others (1964) and Khattab (1969), which were excellent reconnaissance efforts ham-

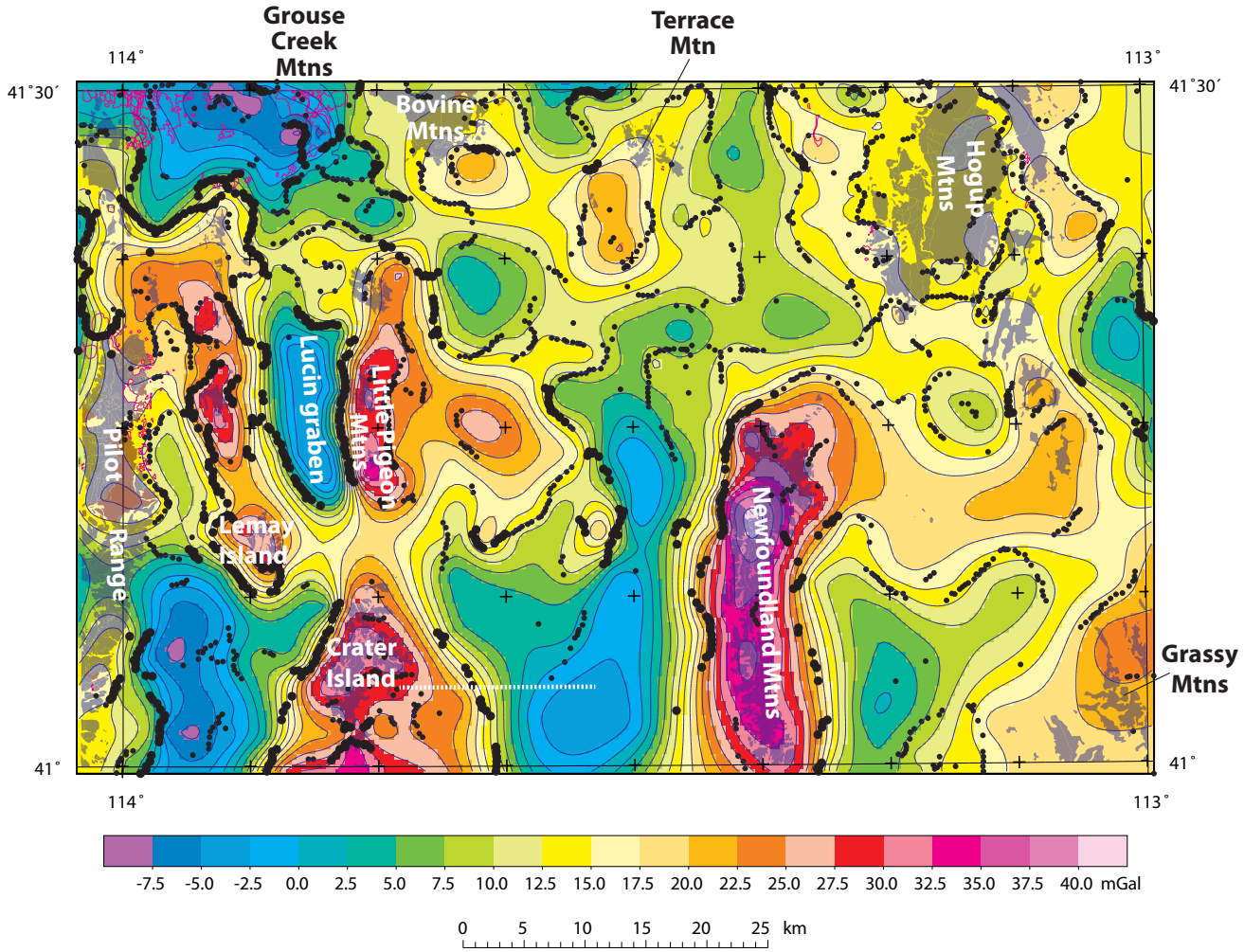

Figure 8. *Isostatic gravity map of Newfoundland Mountains map area. Contour interval is 2.5 mGal. Gray areas are outcrops of pre-Cenozoic basement. Gray-magenta areas are outcrops of Cenozoic plutonic rocks. Magenta lines denote Cenozoic volcanic rocks. Black dots are maximum horizontal gradients (larger circles are those gradients greater than the mean value, smaller circles are those less than the mean value). Dashed white line is the seismic profile (Kim, 1985).*

pered by relatively poor elevation and location control from the available 1:62,500-scale base maps. This map removes the long-wavelength component of the gravity field assuming isostatic compensation, which provides a physics-based regional gravity field. The map incorporates additional measurements, particularly on pre-Cenozoic basement, that provide crucial reference values for estimating basin thickness. Despite these improvements, additional gravity measurements are needed for detailed studies in much of the quadrangle that is very remote and without road access, particularly in the mud flats of the Great Salt Lake Desert.

The magnetic map (figure 9) is based on a fixed-wing aeromagnetic survey flown in 2011 that covers most of the quadrangle and a survey flown in 2010 that covers the northern edge of the quadrangle. Data were not collected in the southeastern part of the quadrangle because of flight restrictions over the Utah Testing and Training Range (UTTR North area). Processing details and data are available in Langenheim (2016).

Magnetic data were collected at a nominal height of 305 meters (1000 ft) above ground along east-west flight lines spaced 800 meters (2625 ft) apart. Note, however, that the average height of the aircraft above terrain was 600 meters (1969 ft), with the aircraft as much as 1900 meters (6234 ft) above the area between the Silver Island Mountains and the Pilot Range and 900 meters (2953 ft) above the areas flanking the tallest parts of the Newfoundland Mountains. Accuracy of this survey is 1 nanotesla (nT) or better. The survey is a considerable improvement on pre-existing data, which consisted of profiles flown 8000 meters (26,247 ft) apart at a constant altitude of 3660 meters (12,008 ft) above sea level (Zietz and others, 1976). The new survey particularly highlights short-wavelength magnetic anomalies associated with Cenozoic volcanic rocks.

To help delineate structural trends and gradients expressed in the gravity and magnetic fields, a computer algorithm was used to locate the maximum horizontal gradient

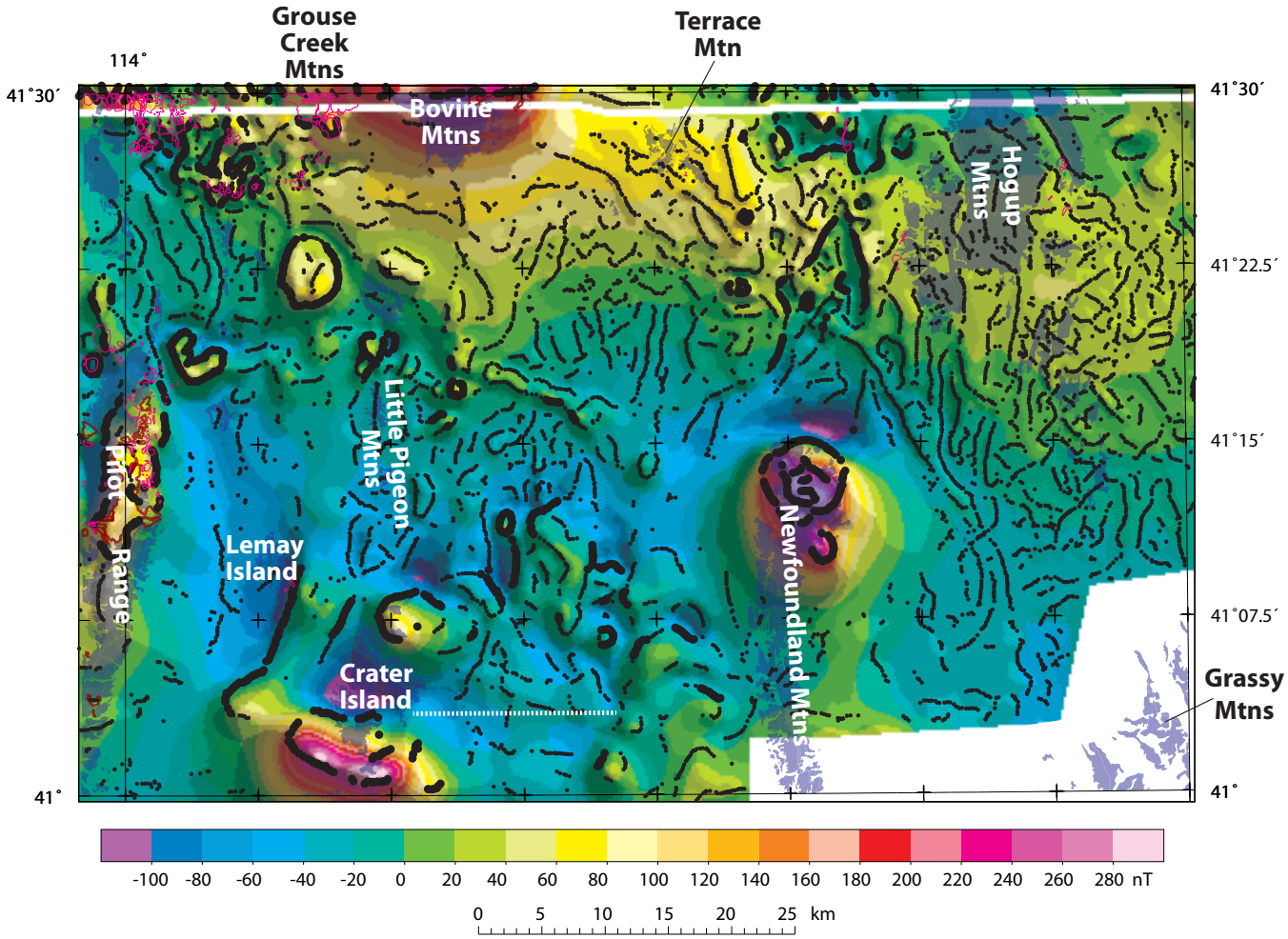

Figure 9. *Aeromagnetic map of Newfoundland Mountains map area. No detailed aeromagnetic data exist in southeastern corner of map (UTTR, North area). White line near northern edge of map denotes boundary between two detailed surveys. Contour interval is 20 nT. Purple-colored areas are outcrops of pre-Cenozoic basement. Brown lines are outcrops of Cenozoic plutonic rocks. Magenta lines denote Cenozoic volcanic rocks. Black dots are magnetization boundaries or maximum horizontal gradients (larger circles are those greater than the mean value, smaller circles are those less than the mean value). Dashed white line is the seismic profile (Kim, 1985).*

(Cordell and Grauch, 1985; Blakely and Simpson, 1986). Concealed basin-bounding faults beneath the valley areas were mapped using horizontal gradients in the gravity and magnetic fields. We calculated magnetization boundaries on a filtered version of the magnetic field to isolate anomalies caused by shallow sources (Blakely, 1995). First the magnetic field was upward-continued 100 meters (328 ft) and subtracted from the original magnetic field. This procedure emphasizes those components of the magnetic field that are caused by the shallow parts of the magnetic bodies, which are most closely related to the mapped geology. Second, the resulting residual aeromagnetic field was mathematically transformed into magnetic potential anomalies (Baranov, 1957); this procedure effectively converts the magnetic field to the equivalent "gravity" field that would be produced if all magnetic material were replaced by proportionately dense material. The horizontal gradient of the magnetic potential field was then calculated. Gradient maxima occur approximately over steeply dipping contacts that separate rocks of contrasting densities or magnetizations. For moderate to steep dips (45˚ to vertical), the horizontal displacement of a gradient maximum from the top edge of an offset horizontal layer is always less than or equal to the depth to the top of the source (Grauch and Cordell, 1987).

To estimate basin thickness, we used the inversion method of Jachens and Moring (1990) and modified to include constraints, such as wells or other geophysical information, in the inversion. The method strives to separate the observed gravity into two components, that produced by variations of density within the pre-Cenozoic basement (figure 10a) and that produced by variations of thickness of the overlying basin deposits. The latter component is directly inverted to provide the thickness of deposits. The density of the basement is allowed to vary horizontally (as constrained by gravity measurements made on basement outcrops), whereas the density of the basin-filling deposits is forced to increase with depth according to a specified density-depth relationship. We used a density-depth relationship (table 1) based on Jachens and Moring (1990) developed from analysis of well and seismic data from Nevada for sedimentary deposits and on McNeil and Smith (1992) based on density logs from wells near Ogden and Brigham City, Utah. This relationship is consistent with densities derived from seismic interval velocities along a seismic line east of Crater Island, at least to depths of about 1 to 1.5 kilometers (0.6 to 0.9 mi) (Kim, 1985).

The calculation is constrained in places where the depth to basement is known from independent measurements. This information comes from two main sources: digital geology (the Newfoundland Mountains map; plate 1) and a handful of deep wells (table 2). The inversion results in two products: the gravitational attraction of the basement (figure 10a), and the thickness of basin-filling deposits (figure 10b).

It is important to understand the limitations of the gravity inversion. This calculation is regional in scope and, as such, is intended to highlight the regional distribution of basins and their relative depths and shapes. We have grayed out areas where the sparse distribution of measurements limits even a regional understanding of basin geometry (figure 10b). Unfortunately, the paucity of gravity measurements does not allow us to evaluate or incorporate the presence of a west-dipping normal fault near the eastern end of the seismic line of Kim (1985).

Where there are sufficient gravity measurements, the shapes and relative depths of basins yielded by this method are generally reliable, but the calculated thickness of basin-filling deposits is critically dependent on the density-depth function. The inversion presented here does not account for lateral variations in the density distribution of the Cenozoic deposits; the density of basin-filling deposits can and does vary from basin to basin and within individual basins. Densities of basin-filling deposits below a kilometer or two are poorly understood, and the details of the deeper parts of basins should be viewed accordingly. Finally, basin depths may be in error because of poorly known basement gravity variations. For example, a low-density pluton directly beneath a basin may be incorrectly interpreted by the calculation as thicker accumulations of low-density basin deposits. This problem may be of special concern in areas where felsic volcanic deposits are abundant (e.g., in the northwest corner of the map). The absence of measurements on small outcrops of basement about 10 kilometers (16 mi) east of the Newfoundland Mountains also limits our understanding of basement gravity anomalies.

Gravity Anomalies

Isostatic residual gravity anomalies, not surprisingly, show higher values over exposed pre-Cenozoic rocks, particularly over the Newfoundland and Little Pigeon Mountains, and Lemay and Crater Islands (figure 8). Gravity values measured on equivalent basement exposed in the Pilot Range, Hogup, and Grouse Creek Mountains, however, are as much as 10 to 20 milligals (mGal) lower than those measured over those in the Newfoundland Mountains, as highlighted in the basement gravity map (figure 10a). The basement gravity high in the central part of the map area extends from the northwest part of the quadrangle east-southeast across the entire quadrangle. Thicker crust in the northern part of the quadrangle might explain the southward increase in gravity values, given that estimates of crustal thickness from teleseismic receiver function data, although sparse, suggest that the crust thins to the south in this region west of the Great Salt Lake (Lowry and Perez-Gussinye, 2011). Lower values in the Pilot Range may also result from more felsic middle and upper crust than the rest of the quadrangle. Crustal Vp/Vs ratios derived from teleseismic receiver function data are somewhat lower along the western margin of the quadrangle and are interpreted to reflect quartz-rich compositions (Lowry and Perez-Gussinye, 2011), perhaps reflected by Eocene

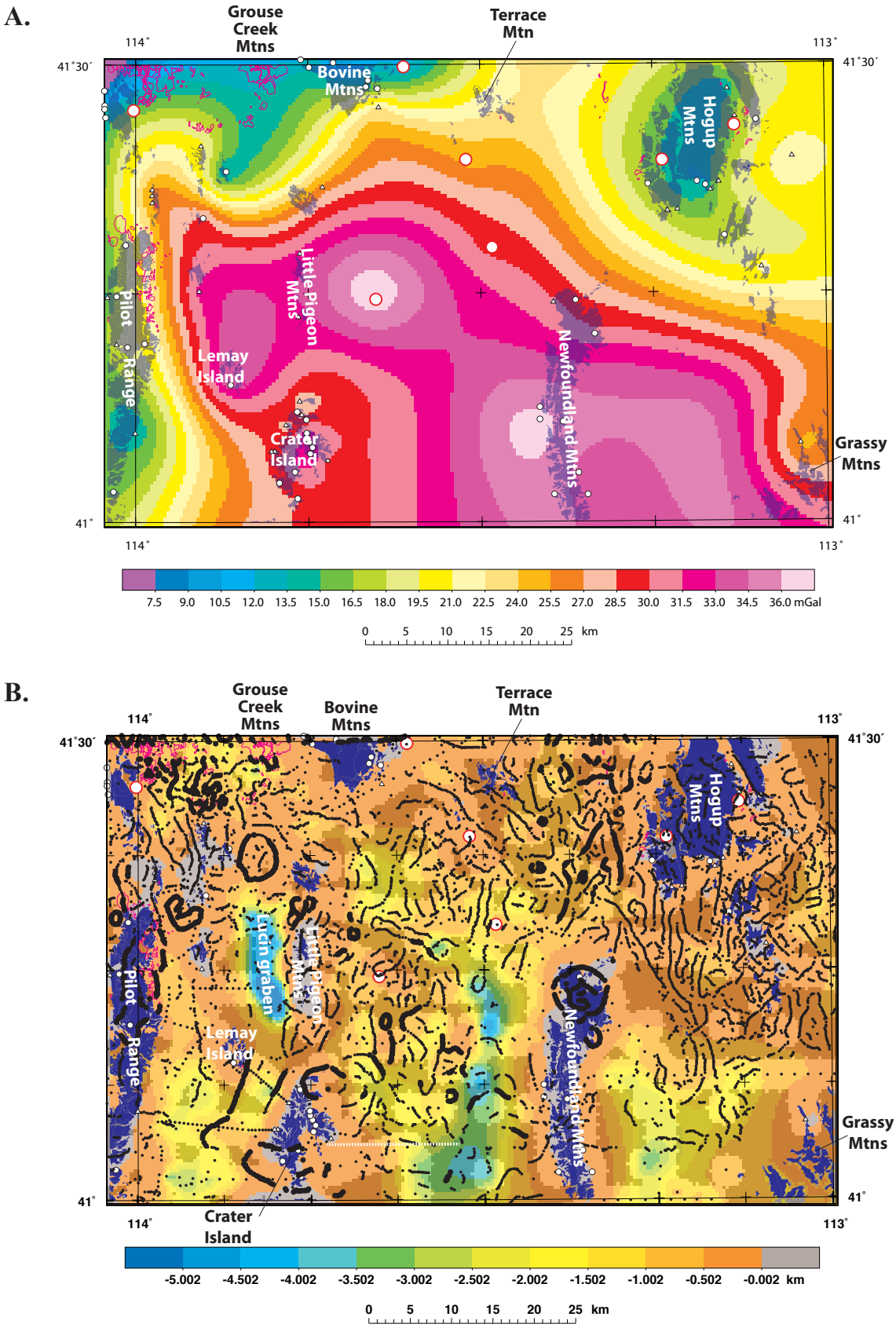

Figure 10. A) *Basement gravity map.* ***B)*** *Basin depth. Purple-colored areas denote outcrops of pre-Cenozoic basement, magenta lines are outcrops of Cenozoic volcanic rocks, red-rimmed white circles are wells that penetrated basement, black-rimmed circles are gravity measurements on basement, and black-rimmed triangles are gravity measurements that are close to basement outcrops. In B), black dots are magnetic maximum horizontal gradients (larger circles are those gradients greater than the mean value, smaller circles are those less than the mean value). Areas not constrained by gravity measurements (small black dots) within 4 km are grayed out. Dashed white line is the seismic profile (Kim, 1985).*

and Miocene rhyolites and dacites (units Ttc, Trd, Tr, and Td) and Eocene monzogranitic to granodioritic intrusions (units Tm and Tbc). This may also explain low values over the southern Grouse Creek and Bovine Mountains that are underlain, in part, by the Emigrant Pass intrusion (unit Teg), which is dominantly monzogranite. The low basement values over the Hogup Mountains may reflect thick sequences of Permian and older sedimentary cover.

Superposed on the basement gravity field are local gravity lows that we attribute to Cenozoic deposits (figure 8). Several of these lows are elongated in a north-south direction, with steep gradients that we, like Cook and others (1964), consider to reflect basin-bounding faults, such as those bounding the Lucin graben west of the Little Pigeon Mountains. Cook and others (1964) modeled this low as a basin about 2 kilometers (1.2 mi) deep using a constant density contrast of -0.5 g/cm^3. Our inversion for basin thickness (figure 10b) suggests that the basin may be as much as 5 kilometers (3 mi) deep, because the amplitude of the gravity low we measured is greater and our average density contrast is lower. Other significant basins are west and east of the Newfoundland Mountains (2–3 km [1.2–1.8 mi] deep), east of the Pilot Range (2–3 km [1.2–1.8 mi] deep), and west of the Grouse Creek Mountains (1–2 km [0.6–1.2 mi] deep). Many of these basins have north- to northeast-trending margins, perpendicular to the least principal horizontal stress axis for Basin and Range extension, and likely reflect normal faulting.

Table 1. *Density-depth relationship.*

Depth range in meters	Density contrast in kg/m^3
0–600	-550
600–1200	-400
>1200	-250

The existing distribution of gravity measurements is not sufficient to map the geometry of basins beneath much of the Great Salt Lake Desert in detail. However, comparison of the basin depth map, where constrained by gravity measurement, with magnetic gradients (figure 11) suggests that the magnetic gradients may help map structures that are poorly resolved by the gravity data. For example, two gravity traverses across the western margin of the Lucin graben indicate that steep gradients curve toward the southeast (where there are no gravity measurements). The magnetic gradients instead indicate that the western edge of the basin trends north-south (with a possible 1–2 km [0.6–1.2 mi]) step to the east between the two gravity traverses) to connect with the basin between Lemay Island and Crater Island. The western margin of the deep basin west of the Newfoundland Mountains appears to follow a north-northeast-trending set of magnetic gradients that confirm that the seismic profile of Kim (1985) did not extend far enough east to intersect the west Newfoundland graben, but instead may have crossed the western margin of an intrabasinal high beneath the Great Salt Lake Desert, as shown on section A-A'. The gradients also suggest that west-northwest-striking structures may contribute to variations in basin thickness, such as the ridge extending west-northwest from the southern part of Crater Island and the apparent northern termination of the deep basin west of the northern Newfoundland Mountains.

Aeromagnetic Anomalies

Magnetic anomalies are caused by magnetite-bearing rocks, which are generally igneous (figures 9 and 11). We measured magnetic susceptibilities of various rock types exposed throughout the quadrangle. The sedimentary rocks and deposits of Proterozoic to Quaternary age are in general weakly magnetic and are reflected by the featureless, relatively flat magnetic field over areas with extensive sedi-

Table 2. *Wells that penetrated basement.*

Well name	Longitude (NAD27)	Latitude (NAD27)	Total depth in feet (m)	Basement depth in feet (m)
439886[a]	-114.002888	41.450169	640 (195)	420 (128)
433684[a]	-113.131179	41.432440	500 (152)	100 (31)
433242[a]	-113.236066	41.394685	1300 (396)	20 (6)
434841[a]	-113.611003	41.497427	370 (113)	120 (37)
Lemay[b]	-113.4833	41.3	2502 (763)	2108 (643)
4300310412[c]	-113.65225	41.24355	2894 (882)	1280 (390)*
4300320094[c]	-113.52092	41.39585	9077 (2767)	445 (136)

[a] Utah Division of Water Rights. Well name corresponds to WIN number in online database.

[b] Heylmun (1965). Approximately located.

[c] Utah Division of Oil, Gas and Mining. Well name corresponds to API number in online database.

* Cook and others (1964) interpreted this well as having penetrated Paleozoic (?) limestone at 2300 ft, noting that such a thickness results in a much greater total gravity relief between this well and Paleozoic rocks exposed to the west in the Little Pigeon Mountains as was documented at the time. New gravity data in the Little Pigeon Mountains do not resolve the issue. Another plausible pick on basement is at 1280 ft, which we adopt here.

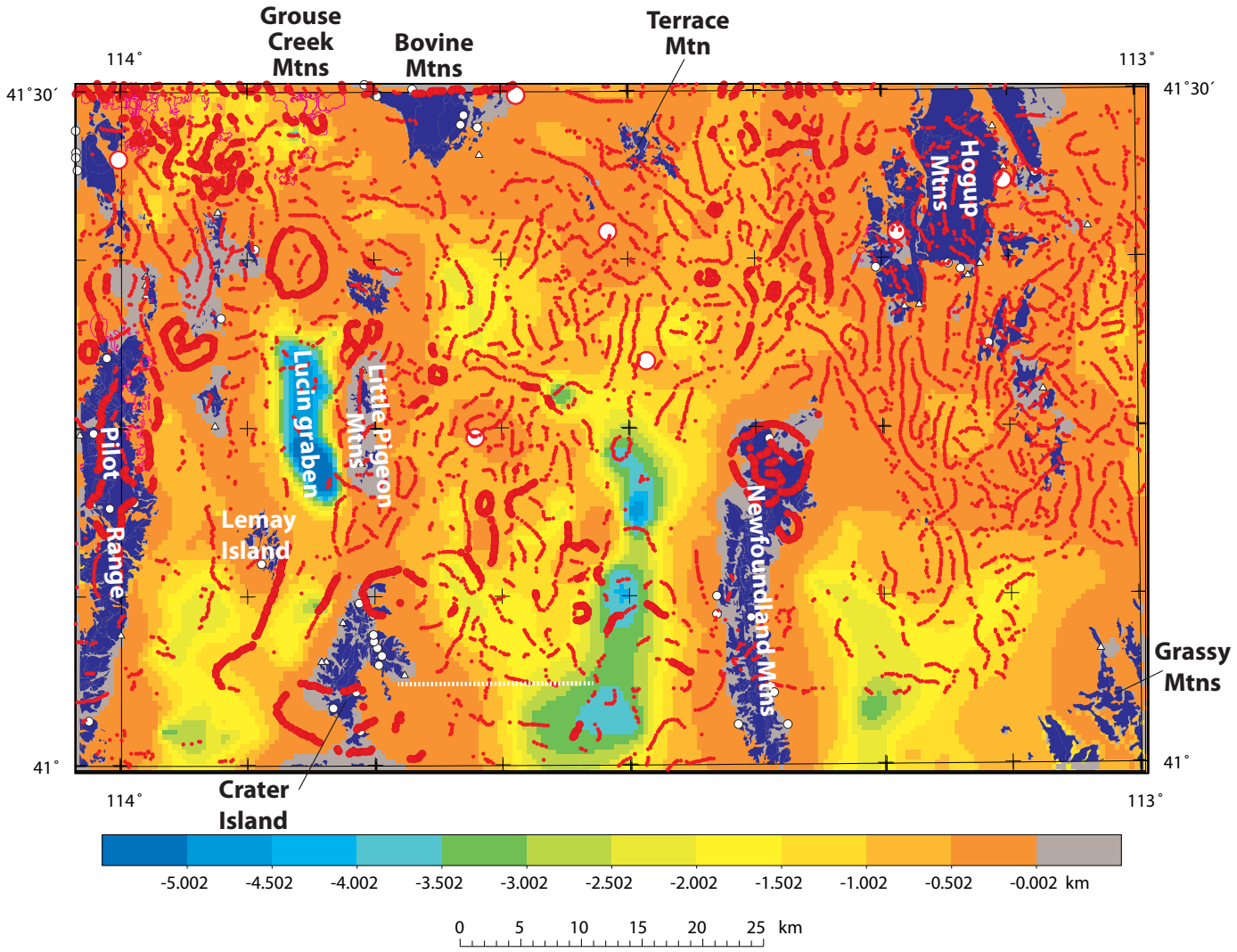

Figure 11. *Basin depth map with magnetization boundaries in red. Dark blue areas denote outcrops of pre-Cenozoic basement, magenta lines are outcrops of Cenozoic volcanic rocks, red-rimmed white circles are wells that penetrated basement, black-rimmed circles are gravity measurements on basement and black-rimmed triangles are gravity measurements that are close to basement outcrops. Dashed white line is the seismic profile (Kim, 1985).*

mentary outcrops, such as the Paleozoic rocks exposed in the Hogup Mountains and southern Pilot Range. In contrast, Cenozoic volcanic rocks are by far the most magnetic rocks exposed in the quadrangle. Volcanic rocks, such as those exposed in the northern Pilot Range, rhyolite and dacite in the northwest corner of the quadrangle, and scraps of basalt west of the Hogup Mountains coincide with prominent, short-wavelength magnetic anomalies. These anomalies are enhanced by magnetization boundaries that form a characteristic "worm-like" pattern. Using this pattern as a guide, the extent of magnetic rocks beneath surficial cover can be mapped. The magnetic data thus predict that volcanic rocks are concealed across the northern part of the map area, from the Pilot Range to the Hogup Mountains, and farther south in the area west of the Newfoundland Mountains (see cross section A-A'). The Lemay well (plate 1) intersected volcanic flows between 515 and 643 meters (1690 and 2110 ft), interpreted by Heylmun (1965) as being the "Lower Volcanic Sequence," thought to be Oligocene at the time. Along a seismic profile some 30 kilometers (19 mi) to the south, Kim (1985) correlated a layer characterized by diffractions and incoherent reflections to the volcanic rocks found in the Lemay well. Such an interpretation is plausible, given the complicated magnetic pattern between the seismic line and the Lemay well.

The magnetic anomalies associated with the volcanic rocks can also provide information on the polarity of the magnetization and can help confirm independently the ages of some of the volcanic units. The basalt exposed at Sheep Mountain (unit Qb, east of Terrace Mtn., plate 1), dated at 1.1 ± 0.1 Ma (Miller and others, 1995), coincides with a localized magnetic high (figure 9), indicating that the basalt is of normal polarity. The latter age places the unit near the cusp of a short normal polarity between 0.99 and 1.07 Ma (Cande and Kent, 1995). If the age range of the normal polarity is cor-

rect, the age of the basalt lies within the younger range of the isotopic age uncertainty. Another basalt (unit Tby, plate 1) exposed 15 kilometers (9 mi) to the southeast, immediately west of the Hogup Mountains, coincides with a subtle magnetic low. Its age of 4.3 ± 0.3 Ma (Miller and others, 1995) places it within a reversed polarity chron between 4.29 and 4.48 Ma (Cande and Kent, 1995). The Rhyolite Butte flow (unit Tr) at the north end of the Pilot Range (plate 1) straddles a magnetic high to the east and a magnetic low to the west (figure 9) and was dated by Armstrong (1970) at 8.6 ± 0.2 Ma (recalculated K-Ar age) and by Miller (unpublished) at 8.8 ± 0.3 Ma. The permissible age range spans both normal and reversed polarity chrons, whereas a reasonable average of the two ages (8.7 ± 0.2 Ma) places the flow within a normal polarity chron. The high may reflect superposition of another concealed rhyolite flow or deeper source within the basement that extends 5 kilometers (3 mi) north of the rhyolite outcrop. The pronounced magnetic low coincident with the basalt at Black Butte (unit Tbi, exposed on the northwestern side of the Pilot Range) indicates that the basalt is reverse polarity. The flow has a K-Ar plagioclase age of 10.6 ± 1.1 Ma (Miller unpublished) spans multiple polarity chrons of varying length, with a significant normal polarity chron from 9.920 to 10.949 Ma. This suggests that basalt may have been erupted during the younger or older part of the age uncertainty. Other anomalies of interest are the prominent magnetic highs in the extreme northwestern corner of the map that coincide with rhyolite and dacite flows (units Tr and Td), and the magnetic low that coincides with rhyodacite exposed in the eastern part of Lemay Island (unit Trd).

Other anomaly producers include late Eocene intrusive rocks and Jurassic plutons (figures 9 and 11). In particular, significant magnetic highs coincide with the Jurassic Newfoundland stock (unit Jn) and the Crater Island quartz monzonite (unit Jc), and another somewhat less intense high is associated with the granodiorite at the northern end of Crater Island (unit Jgd). The Crater Island quartz monzonite appears to be elongate in a west-northwest direction and extends about 5 kilometers (3 mi) in both directions beyond its exposed extent. The Newfoundland stock can be considered to be a semi-circle centered about 3 kilometers (2 mi) north of Desert Peak (plate 1). Two smaller outcrops of the Newfoundland stock about 2 kilometers (1 mi) to the southeast produce less prominent magnetic anomalies. Magnetic highs are also associated with the late Eocene Emigrant Pass and McGinty plutons (units Teg and Tm, respectively), although these anomalies appear to be superposed on broader magnetic highs that spill over outcrops of weakly magnetic rocks. For the McGinty pluton, the most pronounced part of the high also includes outcrops of Miocene diabase (Tdb) that are faulted along the east flank of the pluton whereas to the south of the pluton, the high broadens and diminishes in amplitude towards small outcrops of other Tertiary and Jurassic plutonic rocks (units Tbc, Tg, and Jms). The Jurassic Miners Spring granite (unit Jms) is likely weakly magnetic because of its two-mica composition.

The Emigrant Pass pluton (unit Teg), in particular, is located on a magnetic high that extends across weakly magnetic Paleozoic sedimentary rocks in the Bovine Mountains (figure 9). The pluton also lies at the southern end of a broad, long-wavelength magnetic high that trends north of the quadrangle across the Grouse Creek Mountains, encompassing both weakly magnetic Archean granite and outcrops of Salt Lake Formation as well as a very broad magnetic high that trends east-southeast across the northern part of the quadrangle toward the southern end of the Hogup Mountains. The extent of the high in the Bovine Mountains could be interpreted as a greater volume of Emigrant Pass granite. Measured magnetic susceptibilities of the Emigrant Pass pluton, however, are considerably less than the Cenozoic volcanic rocks so a more likely explanation for the very broad magnetic high extending across the northern end of the quadrangle is a completely buried unit within the Archean basement. This broad magnetic high also roughly coincides with lower basement gravity values and may reflect a deeper-seated structure that separates deeper extensional basins south of the structure from shallower basins to the north. It lies north of the accommodation zone (described in the section on Structure) inferred from basin geometries and terrane mismatches.

The aeromagnetic data allow evaluation of proposed intrusions. Miller and McCarthy (2002) suggested that the gravity high southwest of Terrace Mountain (figure 8) is due to a shallow mafic intrusion that could account for brecciation and metamorphism observed in small outcrops of Permian strata. The lack of a corresponding magnetic high argues against such an interpretation unless the mafic intrusion is not magnetic. Other anomalies, however, could reflect buried intrusions, such as the horseshoe-shaped and oblong anomalies about 5 kilometers (3 mi) and about 15 kilometers (9 mi) northeast of the Pilot Range, respectively.

Filtering of the magnetic data to enhance those anomalies caused by shallow sources reveals subtle gradients in areas with exposed, weakly magnetic rocks. For example, north-trending gradients are present over weakly magnetic Paleozoic sedimentary rocks of the Hogup Mountains. These weak gradients are parallel to mapped faults and provide a means to map structural grain elsewhere in the quadrangle. The north-trending pattern extends south from the Hogup Mountains where it is interrupted by a northwest-trending gradient (figures 9 and 11). The northwest-trending gradient projects southeastward toward scattered small outcrops of Paleozoic rocks that are unlike those exposed to the west in the Newfoundland Mountains and thus one interpretation is that this gradient reflects an inferred thrust fault that juxtaposes these two different stratigraphic sequences (plate 1). An alternate interpretation is that the northwest-trending gradient reflects structure within concealed volcanic rocks as the gradient appears to cross the more westerly-trending accommodation zone discussed in the next section.

STRUCTURE

Rocks of the Newfoundland Mountains map area have complex structural histories. Widespread unconformities (Allmendinger and Jordan, 1984; Miller and others, 1991) reflected in stratigraphic sections younger than the Devonian from the Pilot Range to the Newfoundland Mountains must have been formed by Devonian to Permian faulting, but no structures specific to these tectonic events are known in the map area.

After deposition of the stratigraphic sequence ended in the Triassic, rocks in the Newfoundland quadrangle underwent protracted, and incompletely recorded, tectonism. The Pilot Range has a more complete and longer structural history than other parts of the quadrangle because its rocks underwent both ductile and brittle deformation and thus a wide range of igneous and metamorphic rock chronology is possible. The Crater Island and Newfoundland ranges to the east share elements of this structural history, but other ranges have scarce structural chronology or, in the case of the Bovine Mountain area, share a history with the Grouse Creek metamorphic core complex (Compton, 1983). In the following section we briefly describe the Pilot Range structural history and probable related structures in other ranges in the quadrangle.

Rocks of the Pilot range are divided by the Pilot Peak detachment fault into footwall and hanging wall tectonic packages (Miller, 1990b; Miller and Lush, 1994). During the Late Jurassic (~170–155 Ma) igneous rocks were emplaced as synkinematic sheets, dikes, and small plutons into Neoproterozoic and Cambrian metamorphosed strata of the footwall. Metamorphism was at lower amphibolite to upper greenschist facies and rocks acquired pervasive foliation nearly parallel to bedding followed by northwest-dipping foliation. The early foliation has an associated east-oriented lineation and is probably related to thrust faulting; the second foliation has a northeast-oriented lineation. Macroscopic folds associated with the second foliation include major and minor folds that are overturned to the southeast. Bedding-plane faults are spatially associated with disharmonic folds of all scales, accommodating changes in strain across discontinuities. Metamorphic fabrics are expressed in the ~160 Ma Miners Spring pluton. Many metamorphic minerals cooled during the Late Cretaceous, although interpretation as a possible 100-million-year-long metamorphic period versus repeated metamorphic events remains unresolved. In rocks of the hanging wall to the (future) Pilot Peak detachment fault, bedding plane faults that dip gently east with respect to bedding are associated with east-verging folds. Many faults cut out section, but in Mississippian and Devonian sections minor thrust faults occur as well. East of the Pilot Range, thrust faults and low-angle normal faults are associated with Jurassic plutons in Crater Island and Newfoundland Mountains faults (Allmendinger and Jordan, 1984; Miller and others, 1987; Miller, 1990b; Miller and Allmendinger, 1991; Miller and Hoisch, 1995). A significant thrust fault probably lies concealed east of the Newfoundland Mountains where a sharp contrast in Permian rocks (Allmendinger and Jordan, 1984) is most readily explained as juxtaposition by a major thrust fault.

During the Eocene (~42–36 Ma) plutons were emplaced and extensive volcanic accumulations formed at the surface. The Pilot Peak detachment fault formed, placing slightly metamorphosed hanging wall rocks onto the metamorphic rocks of the south-central Pilot Range (Miller, 1985; Miller, 1990b). Plutons emplaced below and across the detachment fault have weak ductile fabrics overprinted by fractures and associated greenschist grade mineralization. The weak ductile fabrics in adjacent rocks crosscut all higher grade fabrics. Folded and sheared rock in the Pilot Peak detachment fault is cut by Eocene plutons (plate 2, cross section A-A'). The detachment fault cuts across major footwall folds but probably was a west-dipping fault with respect to overall stratigraphy. The Eocene Pilot Peak detachment fault can be shown to have at least 6.4 kilometers (4 mi) of throw in a westward direction by the juxtaposition of Paleozoic rocks over unlike Proterozoic rocks. This measurement, from just south of Patterson Pass (figure 1), is where the Eocene detachment fault was intruded by the McGinty pluton (unit Tm). In hanging wall rocks, low-angle normal faults are common; they dip west with respect to bedding and predate Eocene plutons and dikes. East of the Pilot Range, normal faults may be related to this Eocene extension? episode.

During the Miocene (~20–10 Ma) sedimentary basins and volcanic rocks developed regionally (Cook and others, 1964, 1989). Associated west-dipping normal faults are related to a reactivated Pilot Peak detachment fault that represents continued top-to-the-west detachment. Older faults may be rotated in panels bounded by normal faults that root downward into the detachment. The detachment cuts the top of the McGinty Pluton as well as a thick Salt Lake Formation section, which is rotated to nearly vertical dips. The Miocene Pilot Peak detachment fault can be shown to have at least 4.8 kilometers (3 mi) of throw in a westward direction by the juxtaposition of Paleozoic rocks over unlike Eocene plutonic rocks near Copper Mountain. Some Miocene faults, such as those along the eastern side of the Pilot Range, are partly exposed and vary from steep to gentle dip along strike (Miller, 1993; Miller and others, 1993). Basin margins inferred from gravity gradients appear to correspond, in that gentle gradients (and shallow basins) are associated with gentler dips on the normal faults (for example, northwest of Lemay Island). Although in places the detachment fault may steepen into range-front faults, in detail in many places it is cut by a younger set of Pliocene-Quaternary(?) steep faults along both sides of the Pilot Range. Similar steep? range-bounding faults exist eastward across the quadrangle.

Widespread late Pleistocene and Holocene sediment is well exposed in many places and is generally not cut by faults, suggesting that late Quaternary earthquakes have not produced surface rupture in much of the map area. However, scarps in Pleistocene deposits and structural relief along the

Pilot Range and Hogup Mountains support potentially active Quaternary faulting in these parts of the map area.

Structural highs separated by gravity lows form five main north-trending structural blocks (figures 1 and 8). From west to east these blocks are: (1) the Pilot Range, (2) a belt of small hills (Lemay Island, Lion Mountain) that coincides with a gravity high that we infer represents a continuous block of Paleozoic rocks, (3) Crater Island likewise is connected with the Little Pigeon Mountains and Pigeon Mountain, (4) a structural high that is shallowly buried by Cenozoic sediments lies about half way between the Little Pigeon Mountains and the Newfoundland Mountains (plate 2, cross section A-A'), and (5) the Newfoundland Mountain block. East of the Newfoundland Mountains gravity data are too sparse to evaluate whether one or more buried horsts lie between the Newfoundland and Grassy Mountains. The second structural block terminates southward at Pilot Valley playa, and the normal fault on its west side may strike southeastward toward Silver Island (south of Crater Island; figure 1), cutting off the western end of the magnetic anomaly associated with the Crater Island quartz monzonite (figure 9).

All structural blocks are bounded on the north by an approximately east-southeast-trending zone, north of which lie mostly Cenozoic and uppermost Paleozoic strata in mountains that are separated by basins that do not correspond to basins to the south. Within this northern area, the structure of basins may be influenced by several mapped Cenozoic low-angle normal faults (Compton, 1983; Jordan 1983; Todd, 1983; Miller and Oviatt, 1994; McCarthy and Miller, 2002), and upper Paleozoic strata in many mountains differ significantly from age-equivalent strata to the south. For instance, Permian and Pennsylvanian strata of the Hogup and Grassy Mountains, although broadly similar, have many specific differences (compare Stifel, 1964, and Doelling, 1964). Permian rocks in Terrace Mountain are unlike those in the Newfoundland Mountains. We interpret the zone as an accommodation zone as defined by Faulds and Varga (1998), across which Miocene normal faults (and older structures) are mismatched. The zone accommodates the mismatch through rotation, lateral ramps between normal and thrust faults, and more complex faulting. Along the reach from Terrace Mountain to the Hogup Mountains, the zone appears to be 3 to 5 kilometers (2-3 mi) wide and composed of faults somewhat oblique to the overall trend, if our interpretation of gravity anomalies is correct. In this same area, magnetic patterns suggest that volcanic rocks lie in the shallow subsurface and appear to cross the zone. Exposed rocks associated with this magnetic pattern between Terrace Mountain and the Hogup Mountains are Pliocene to Quaternary in age. These inferences lead to the suggestion that the accommodation zone ceased activity before the Pliocene. The accommodation zone narrows westward, where it lies between Paleozoic strata north of Grouse Creek Junction and rhyolite flows just 1 kilometer (0.6 mi) to the north, and then arcs to a west-southwest trend as it continues west between Ordovician strata of Gartney Mountain and Permian strata of the southern terminus of the Goose Creek Mountains. Major north-trending folds that verge to the east exist at the Bovine, Terrace, and Hogup Mountains; these may be counterparts to Jurassic folds farther south. Eocene and Miocene detachment faults and low-grade metamorphism are documented at the Bovine Mountains. The accommodation zone probably formed during the Mesozoic as a series of lateral ramps during thrust faulting and was modified during the Cenozoic as a boundary between provinces of different extensional histories.

DESCRIPTION OF MAP UNITS

QUATERNARY-TERTIARY SURFICIAL DEPOSITS

Qu **Surficial deposits, undivided** (Holocene and Pleistocene) – Cross section only.

Alluvial Deposits

Qam **Alluvial mud** (Holocene) – Mud around margins of broad flats of Great Salt Lake Desert, distinguished from playa mud by presence of stream channels. May include eroded lacustrine marl. Also present in depressions bounded by lacustrine beaches. About 2 to 30 meters (6–100 ft) thick.

Qal **Stream Alluvium** (Holocene) – Gravel, sand, silt, and mud deposited in active washes. In many stream channels below elevations of approximately 1430 meters (~4700 ft), consists primarily of reworked lacustrine marl. About 2 to 3 meters (6–10 ft) thick.

Qafy **Young alluvial-fan deposits** (Holocene) – Gravel, sand, and silt forming alluvial cones and fans, many overlying deposits of Lake Bonneville. Locally, includes thin deposits of lacustrine marl, silt, and gravel that preserve shorelines of Lake Bonneville in places. About 2 to 6 meters (6–20 ft) thick.

Qafo **Older alluvial-fan deposits** (Pleistocene) – Moderately consolidated, poorly sorted gravel, sand, and silt forming broad fans mainly among mountains in western part of map area. Largely predates Lake Bonneville shorelines and deposits, although youngest deposits may be coeval with Lake Bonneville. About 2 to 6 meters (6–20 ft) thick.

QTaf **Oldest alluvial-fan deposits** (Pleistocene and Pliocene?) – Moderately consolidated, poorly sorted bouldery gravel and sand in deeply eroded alluvial-fan deposits on flanks of Pilot Range. About 6 to 60 meters (20–200 ft) thick.

Playa and Spring Deposits

Qpm **Playa mud** (Holocene) – White, tan, and gray carbonate mud, oolitic sand, and gypsum and halite evaporite deposits of dry and discharging playas of Pilot Valley and Great Salt Lake Desert. Locally used for commercial evaporation. About 1 to 9 meters (3–30 ft) thick (Nelson and Rey, 2018).

Qsm **Spring mud** (Holocene) – Dark-colored, organic-rich mud and sand in heavily vegetated areas surrounding freshwater springs. About 2 to 3 meters (6–10 ft) thick.

Lacustrine and Mixed-Environment Deposits

Qlm **Lacustrine marl** (Pleistocene) – White, pale-brown to pink, and gray marl and clay of offshore Lake Bonneville. Locally contains considerable silt deposited in nearshore environment[?]. As mapped, locally includes platy, cemented ooid deposits at base and top. About 2 to 10 meters (6–30 ft) thick.

Qli **Lacustrine silt** (Pleistocene) – Light-colored silt, clay, and fine sand deposited in nearshore Lake Bonneville. About 2 to 6 meters (6-20 ft) thick.

Qls **Lacustrine sand** (Pleistocene) – Well-sorted, fine to coarse sand. Deposited in Lake Bonneville adjacent to barrier beaches or as shorezone deposits near local sand source. Also mapped in broad low-gradient platforms south of Terrace Mountain and adjacent to Newfoundland Mountains, where alluvial veneer is included. About 2 to 6 meters (6–20 ft) thick.

Qlg **Lacustrine gravel** (Pleistocene) – Cobble- and pebble-gravel and subordinate sand. Forms prominent barrier beaches, spits, and tombolos. About 2 to 6 meters (6–20 ft) thick.

Qla **Lacustrine and alluvial deposits, undivided** (Pleistocene) – Thin lacustrine deposits on older alluvium. Typically represents wave-eroded older alluvial-fan deposits (Qafo) mantled by thin strips of lens-shaped bodies of sand and gravel. About 0.5 to 3 meters (1–10 ft) thick.

Eolian Deposits

Qei **Eolian silt** (Holocene) – Silt, fine sand, and clay deposited as an eolian blanket less than 1 meter (3 ft) thick; locally reworked by streams. Most deposits on broad plain in northeastern part of quadrangle east of Sheep Mountain.

Qes **Eolian sand and silt** (Holocene) – Dunes and sheets of brown sand and silt, generally less than 3 meters (10 ft) thick.

Qeo **Eolian ooid sand** (Holocene)– Dunes and sand sheets composed of ooids. Mostly in dunes fringing Great Salt Lake Desert. Many dunes are rounded by wave action of shallow lakes. About 2 to 15 meters (6–50 ft) thick.

Qem **Eolian mud** (Holocene) – Dunes and sand sheets composed of mud pellets, mainly present near Newfoundland and Grassy Mountains. Mostly reworked from playa flats. Many dunes are rounded by wave action of shallow lakes. About 2 to 3 meters (6–10 ft) thick.

Mass-Movement Deposits

Qmc **Colluvium and talus** (Holocene) – Unconsolidated colluvial materials on steep slopes, mostly in the western part of the quadrangle. About 2 to 3 meters (6–10 ft) thick.

Qms **Landslide deposits** (Holocene and Pleistocene) – Displaced deposits of disaggregated rock and alluvium that form hummocky terrain. About 2 to 3 meters (6–10 ft) thick.

Quaternary Volcanic Rocks

Qb **Basalt of Sheep Mountain** (Pleistocene) – Dark-brown to black basalt flows forming low hills in vicinity of Sheep Mountain. Locally thermally oxidized and scoriaceous. Plagioclase and olivine occur as phenocrysts and glomerocrysts in dark-gray matrix. K-Ar whole-rock age is 1.13 ± 0.11 Ma (Miller and others, 1995). About 6 to 20 meters (20–60 ft) thick.

Tertiary (Neogene) Igneous and Sedimentary Rocks

Tby **Younger basaltic lava flows** (Pliocene) – Dark-brown to black basalt containing pyroxene, amphibole, olivine, plagioclase, and iron oxide minerals. Generally aphanitic with plagioclase and olivine occurring as small, sparse phenocrysts and glomerocrysts. Flows on western side of Hogup Mountains have weakly developed tumuli and columnar joints, and have a K-Ar whole-rock age of 4.3 ± 0.3 Ma (Miller and others, 1995). Undated flows southeast of Sheep Mountain assigned to this unit based on physical characteristics, stratigraphic relations, and chemistry (table 3). A small flow west of Big Pass in Hogup Mountains (labeled Tby?) is tentatively assigned

Table 3. *Summary of diagnostic major oxide elements for basaltic units.*

Map unit	Age (Ma)	Rock name	Rock chemistry*		
			SiO_2 (%)	TiO_2 (%)	Fe_2O_3 (%)**
Basalt of Sheep Mountain (Qb)	~1	basalt	~46	~3	~16.2
Younger basaltic lava flows (Tby)	~4	basalt and picro basalt	44.5–46	~2.4–3.3	~15.2–17.2
Intermediate-age basaltic lava flows (Tbi)	10.5 to 18.5	basalt, basaltic andesite, trachybasalt	47–57	~0.9–1.6	~9.4–11

* Whole-rock chemistry by wavelength dispersive XRF

** Total Fe as Fe_2O_3

to this unit based on stratigraphic relations. Outcrops of ultramafic rock (tephrite or basanite) that may represent a minette (E.H. Christiansen, verbal communication, 2016) are associated with the basalt southeast of Sheep Mountain. About 6 to 20 meters (20–60 ft) thick.

Ts **Salt Lake Formation, undivided** (Miocene) – Moderately lithified sedimentary and volcanic rocks. Common sedimentary rock types are thin-bedded siltstone, sandstone, shale, limestone, and conglomerate, all commonly tuffaceous, and generally representative of lacustrine conditions. Typically white, yellow, yellowish brown and green in color. Beds of light-gray vitric tuff that was erupted from the Snake River Plain and vents that produced local rhyolite flows are common. Tuffaceous rocks altered to massive brown clay in several places in the Hogup Mountains. Based on dated volcanic flows within the section, unit ranges from greater than 18 Ma to as young as about 8 Ma in the map area. Greater than 5000 meters (15000 ft) thick.

Tsc **Salt Lake Formation, conglomerate** (Miocene) – Moderately lithified, well-sorted pebble conglomerate. East of Pilot Range, unit contains clasts of lineated tectonites. About 9 to 60 meters (40–200 ft) thick.

Tt **Tuff and tuff breccia** (Miocene) – Moderately to well-lithified tuff breccia and welded ash flows of biotite rhyolite composition. Proximal deposits associated with the eruptions that produced the rhyolite and dacite flows exposed in the northwestern part of the map area. Locally very coarse, with clasts of pumice, rhyolite vitrophyre, flow-foliated rhyolite, and basalt to 50 centimeters (20 in). Greater than 70 meters (220 ft) thick.

Tr **Rhyolite** (Miocene) – Resistant, medium-gray, quartz-sanidine rhyolite lava flows. Typically well flow-foliated; crops out with cavernous weathering and prominent joints. Sanidine and feldspar phenocrysts are abundant. About 8 to 14 Ma (Armstrong, 1970; Scarbrough, 1984; Miller and Oviatt, 1994). As thick as 100 meters (330 ft).

Td **Dacite** (Miocene) – Fine- to medium-grained hornblende dacite. Generally strongly flow-foliated. Forms rubbly hills in northwest corner of map area. About 12 to 14 Ma (Miller and Oviatt, 1994). Greater than 70 meters (220 ft) thick.

Tbi **Intermediate-age basaltic lava flows** (Miocene) – Dark-brown to black basalt and basaltic andesite containing pyroxene, amphibole, olivine, plagioclase, and iron oxide minerals. Flows are typically interbedded with Salt Lake Formation and have olivine phenocrysts in aphanitic groundmass. Outcrops vary from fresh and well-preserved to significantly weathered, with olivine altered to iddingsite. Dated flows include Black Butte in the Pilot Range (K-Ar plagioclase, 10.3 ± 1.5 Ma and 10.9 ± 1.1 Ma, Miller unpublished), flows south of Big Pass in the Hogup Mountains (K-Ar whole-rock, 10.4 ± 0.3 Ma, Miller unpublished), and flows near Terrace Mountain (K-Ar whole-rock, 18.3 ± 0.5 Ma and 18.5 ± 0.5 Ma, Miller and McCarthy, 2002). Undated flows interbedded with Salt Lake Formation near Kilgore Spring (far northwestern corner of map area) have been assigned to this unit based on stratigraphic relations. Undated flows southeast of Sheep Mountain (labeled Tbi?) are tentatively assigned to this unit based on physical characteristics and chemistry (table 3), but may be younger because they are not interbedded with Salt Lake Formation and are in proximity to units Qb and Tby. Basaltic lava flows of possible Eocene age are not found in the Newfoundland Mountains map, but do occur about 8 kilometers (5 mi) north of Sheep Mountain where they are mapped by Miller and others (2012) as unit Tbo (Older trachybasaltic lava flows). About 2 to 20 meters (6–60 ft) thick.

Tdb **Diabase** (Miocene) – Dark-brown, coarse- to fine-grained dikes and small bodies of pyroxene amphibole diabase. Intrudes McGinty Monzogranite

and Salt Lake Formation east of Pilot Range so age is younger than about 12 Ma. About 2 to 20 meters (6–60 ft) thick.

Tertiary (Paleogene) Igneous and Sedimentary Rocks

Ttc **Rhyolitic tuff and sedimentary rocks** (Eocene) – White to gray, commonly altered, rhyolite tuff and minor sedimentary rock. Includes probable unwelded rhyolite ash flows, minor welded tuff, and gray air-fall tuff containing pumice, as well as interbedded shale and sandstone, and minor green conglomerate consisting of reworked tuff. Exposed along flanks of northern Pilot Range. Tuff is biotite-hornblende rhyolite to dacite and has K-Ar ages of about 37 Ma (Miller and others, 1993). Greater than 1200 meters (4000 ft) thick.

Trd **Rhyodacite** (Eocene) – Sequence of lava flows at Lemay Island. Contains plagioclase, alkali feldspar, and quartz phenocrysts. A K-Ar age is about 33 Ma (Miller and Glick, 1986), but the unit probably is late Eocene, like similar volcanic and intrusive rocks in the region. Greater than 425 meters (1400 ft) thick.

Tg **Granodiorite dikes** (Eocene) – Hornblende-biotite granodiorite dikes in the Pilot Range. Coarse-grained with very fine grained matrix, white to gray in color. No radiometric age.

Tbc **Bettridge Creek Granodiorite** (Eocene) – Hornblende-biotite granodiorite forming a small pluton in the southern Pilot Range. Foliated in many exposures. Forms wide valleys due to advanced weathering and erosion. About 39 Ma (Miller and others, 1987).

Tm **McGinty Monzogranite** (Eocene) – White to gray, coarse-grained, porphyritic monzogranite to granodiorite in the Pilot Range. Phenocrysts of alkali feldspar are set in coarse-grained matrix of plagioclase, alkali feldspar, quartz, and biotite. K-Ar ages of about 32 and 37 Ma were reported by Miller and others (1990b), who argued that the crystallization age was Eocene.

Teg **Emigrant Pass intrusion of Compton and others (1977)** (Eocene) – White to gray, coarse-grained, porphyritic monzogranite to granodiorite. Phenocrysts of alkali feldspar are set in coarse-grained matrix of plagioclase, alkali feldspar, quartz, and biotite. More mafic parts locally. An Rb-Sr age of about 38 Ma was reported by Compton and others (1977); age revised to 41–32 Ma based on U-Pb study of zircon (Egger and others, 2003; Konstantinou and others, 2013). We consider the part in the Newfoundland quadrangle to be Eocene in age.

Jurassic Plutonic Rocks

Jms **Miners Spring Granite** (Jurassic) – Medium- to pale-gray, fine- to medium-grained, biotite-muscovite granite forming small stocks and networks of dikes in southern Pilot Range. Miller and others (1987) reported a U-Pb zircon concordia age of about 165 to 155 Ma.

Jgd **Granodiorite** (Jurassic) – Zoned pluton in northern Crater Island of light-gray biotite granodiorite and monzogranite. Porphyritic and coarse-grained in outer phase; medium-grained, tri-modal porphyritic in central phase. K-Ar biotite age is about 152 Ma (Miller and others, 1990b).

Jpm **Porphyritic monzogranite** (Jurassic) – Medium-gray, medium- to coarse-grained, subequigranular to porphyritic biotite monzogranite in southern Crater Island. Includes finer-grained granite in extensive dike swarm north of pluton. K-Ar biotite age is about 154 Ma (Miller and others, 1990b).

Jc **Crater Island Quartz Monzonite** (Jurassic) – Medium-gray, coarse-grained, hornblende biotite quartz monzonite in southern Crater Island. Includes mafic phase of hornblende-pyroxene monzodiorite. K-Ar biotite age is about 152 Ma (Miller and others, 1990b).

Jn **Newfoundland Stock of Caroon** (1977) (Jurassic) – Crudely zoned, hornblende-biotite granodiorite to biotite monzogranite. K-Ar mineral ages ranging from 153 to 144 Ma were reported by Allmendinger and Jordan (1989) and Miller and others (1990b), who considered the stock to be Jurassic.

Triassic and Paleozoic rocks of the northern Pilot Range, Lion Mountain, Lemay Island, Pigeon Mountain, and Little Pigeon Mountains

Ŧd **Dinwoody Formation** (Triassic) – Yellow, reddish-gray, and brown, thin- to medium-bedded, impure limestone, calcareous shale, and siltstone. Typically fossiliferous. Forms slopes. Unit about 90 meters (300 ft) thick in a fault block at Pigeon Mountain.

Pg **Gerster Formation** (Permian) – Thick-bedded, dark-gray, shelly limestone, chert, sandstone, and siltstone. Limestone near base contains abundant brachiopods. Forms cliffs and steep slopes. Greater than 240 meters (770 ft) thick at Lemay Island.

Pm **Murdock Mountain Formation** (Permian) – Dark- to pale-brown, thin-bedded chert and cherty dolomite. Typically highly fractured. Where less cherty, consists of yellowish-gray to brown calcareous siltstone and silty limestone, locally fossiliferous. Tongue of Gerster Limestone, consisting of thick-bedded, gray, shelly limestone with abundant brachiopods, lies in upper part of the unit (Wardlaw and others, 1979). About 715 meters (2400 ft) thick at Lemay Island.

Ppm **Phosphoria Formation, Meade Peak Phosphatic Shale Tongue** (Permian) – Light-gray, dark-brown, and black phosphatic shale, yellow-brown siltstone; and minor gray limestone and chert. Thin-bedded, recessive weathering, poorly exposed. About 40 to 105 meters (130–350 ft) thick.

Pgr **Grandeur Formation of the Park City Group** (Permian) – Light-gray sandy dolomite, and medium-brown dolomitic sandstone, fine grained. Medium to thick bedded, cross-laminated. Forms cliffs. About 750 meters (2500 ft) thick at Lemay Island. Queried in northwestern corner where sandstone lacks some distinctive features of the Grandeur.

Ptc **Trapper Creek Formation** (Permian) – Calcareous sandstone, thin to medium bedded. Similar to unit in nearby Leach Mountains of Nevada (Miller and others, 1984). Forms steep slopes, generally poorly exposed. About 200 meters (650 ft) thick in Pilot Range and about 600 meters (2000 ft) thick at Lemay Island.

Pbg **Badger Gulch Formation** (Permian) – Laminated to thin-bedded, platy, dark-gray to black, silty limestone and less common siltstone. Some beds bioclastic, typically containing crinoid fragments, spirifer brachiopods, and fusulinids. In the northern Pilot Range, basal 5 to 10 meters (16–33 ft) as mapped includes structurally thinned rocks of the Third Fork Formation. About 730 meters (2400 ft) thick in Pilot Range.

Ptf **Third Fork(?) Formation** (Permian) – Gray and brown, slope-forming, calcareous, platy sandstone and arkose, and silty limestone. Unit is in stratigraphic position of the Third Fork but differs somewhat lithologically from the type formation. Greater than 220 meters (700 ft) thick in Pilot Range; may be as thick as 500 meters (1500 ft) in Jackson Spring area (Douglas, 1984).

PIPs **Strathearn Formation** (Permian and Pennsylvanian) – Conglomerate composed of pebbles to cobbles of dolomite, limestone, sandstone, and chert in matrix of quartz sand and calcite. Base is a pronounced unconformity (Miller and others, 1991). Forms cliffs. Ranges from 5 to 40 meters (18–130 ft) thick.

IPMdc **Diamond Peak Formation and Chainman Shale, undivided** (Pennsylvanian and Mississippian) – Dark-gray shale, and dark-gray, dark-brown, and black sandstone and conglomerate with vein quartz and chert clasts in arkosic sand matrix. Commonly structurally thinned; varies from 20 to 185 meters (60–600 ft) thick in Pilot Range.

Mtp **Tripon Pass Limestone** (Mississippian) – Platy, dark-gray to black, thin-bedded, silty limestone with subordinate interbeds of calcareous siltstone. Weathers light-gray with a pinkish hue. Time-stratigraphic equivalent to the Joana Limestone (Miller and others, 1991). As thick as 425 meters (1400 ft) in Pilot Range.

Dg **Guilmette Formation** (Devonian) – Medium- and dark-gray and black, medium-crystalline limestone. Fossiliferous; locally dolomitic. Upper part contains quartz sand, and typically is altered to dark-brown and red-brown siliceous breccia in Pilot Range area. Forms prominent cliffs. About 390 meters (1280 ft) thick in Pilot Range.

Ds **Simonson Dolomite** (Devonian) – Alternating black and medium-gray, thick beds of coarsely recrystallized dolomite, typically laminated. Forms ledgey steep slopes. About 365 meters (1200 ft) thick in Pilot Range.

DSd **Thick–bedded dolomite, undivided** (Devonian and Silurian) – Off-white, light- and medium-gray, faintly bedded to structureless dolomite and calcareous dolomite. About 500 meters (1650 ft) thick in Pilot Range.

Oes **Ely Springs Dolomite** (Ordovician) – Medium-gray to black, faintly bedded, fractured calcareous dolomite. About 130 meters (425 ft) thick in Pilot Range.

Oe **Eureka Quartzite** (Ordovician) – White and light-gray orthoquartzite. Well-sorted and well-rounded medium quartz sand grains are indented by pressure solution, and in places are partly recrystallized. Highly fractured in most exposures. About 160 meters (525 ft) thick in Pilot Range.

Opl **Lower Pogonip Group** (Ordovician) – Upper part is massive, light- to medium-gray, slightly silty

limestone forming steep slopes. Locally cherty. Lower part is thinly interbedded blue-gray limestone, gray and brown silty limestone, and brown calcareous siltstone. About 320 meters (1050 ft) thick in Pilot Range. Mapped as the Garden City Formation in previous detailed maps.

Paleozoic and Neoproterozoic rocks of the southern Pilot Range, Crater Island, and Newfoundland Mountains

Pgr **Grandeur Formation of the Park City Group** (Permian) – Sandstone and dolomite similar to that described for northern Pilot Range, but less clastic material present (Miller and others, 1991). Greater than 120 meters (400 ft) thick at Crater Island.

Pp **Pequop Formation** (Permian) – Brown-weathering sandy limestone, cherty limestone, and bioclastic cherty limestone. Thickness about 450 to 550 meters (1500–1800 ft) at Crater Island and Newfoundland Mountains.

Pr **Riepetown Sandstone** (Permian) – Medium- to thick-bedded dolomitic and calcareous quartz sandstone forming brown-weathering cliffs (after Steele, 1960). Bioclastic intervals of limestone and dolomite occur. Not distinguished in the Newfoundland Mountains. About 90 meters (300 ft) thick at Crater Island.

PIPs **Strathearn Formation** (Permian and Pennsylvanian) – Conglomerate composed of pebbles to cobbles of dolomite, limestone, sandstone, and chert in matrix of quartz sand and calcite. Chert decreases eastward. Base marks a prominent unconformity. Rests unconformably on Pilot Shale (unit Dp) in Newfoundland Mountains (Allmendinger and Jordan, 1984), and on younger strata in Crater Island (Miller and others, 1990a). Forms cliffs. Ranges from 5 to 40 meters (16–130 ft) thick in the Newfoundland Mountains.

IPe **Ely Limestone** (Pennsylvanian) – Gray and brown, medium- to thick-bedded limestone, silty limestone, and cherty limestone. Forms cliffs. Greater than 250 meters (820 ft) thick in the Pilot Range.

IPMdc **Diamond Peak Formation and Chainman Shale, undivided** (Pennsylvanian and Mississippian) – Dark-gray shale and dark-gray, dark-brown, and black sandstone and conglomerate with quartz, chert, and feldspar clasts. Commonly structurally thinned; up to 375 meters (1230 ft) thick in the Pilot Range.

Mj **Joana Limestone** (Mississippian) – Dark-gray to black, medium- to thick-bedded, coarse-grained limestone with abundant black chert and crinoid fragments in upper part. Forms cliffs. About 125 meters (410 ft) thick in the Pilot Range.

Dp **Pilot Shale** (Devonian) – Light-gray to pink, thin-bedded to laminated, calcareous siltstone and shale. Present only in Newfoundland Mountains (Unit D of Allmendinger and Jordan, 1989). About 300 meters (980 ft) thick.

Dg **Guilmette Formation** (Devonian) – Medium- and dark-gray and black, medium-crystalline limestone. Fossiliferous; locally dolomitic. Upper part contains quartz sand, and typically is altered to dark-brown and red-brown siliceous breccia in Pilot Range area. Forms prominent cliffs. Unit C of Allmendinger and Jordan (1989). As thick as 550 meters (1800 ft) in the Pilot Range.

Ds **Simonson Dolomite** (Devonian) – Alternating black and medium-gray beds of coarsely recrystallized dolomite, typically laminated. Forms ledgey steep slopes. Unit B of Allmendinger and Jordan (1989). About 355 meters (1165 ft) thick at Crater Island.

DSlm **Lone Mountain Dolomite** (Devonian and Silurian) – Light-gray to buff, coarse-grained, thick-bedded to massive dolomite. Characteristically laminated or mottled. Unit A of Allmendinger and Jordan (1989). About 250 meters (820 ft) thick in the Pilot Range.

DSu **Undivided dolomite and limestone** (Devonian and Silurian) – Undivided rocks in the southern Newfoundland Mountains probably corresponding to the Pilot Shale, Guilmette Formation, Simonson Dolomite, and Lone Mountain Dolomite. About 1100 meters (3600 ft) thick.

Sl **Laketown Dolomite** (Silurian) – Thick-bedded, light to dark tan-gray, mottled dolomite with abundant chert in lower part. Forms steep slopes. About 260 meters (850 ft) thick in the Newfoundland Mountains.

Oes **Ely Springs Dolomite** (Ordovician) – Medium-gray to black, faintly bedded, fractured calcareous dolomite. Forms cliffs to steep slopes. About 180 meters (590 ft) thick in the Newfoundland Mountains.

Oe **Eureka Quartzite** (Ordovician) – White and light-gray orthoquartzite. Well-sorted and well-

rounded medium quartz sand grains are indented by pressure solution, and in places are partly recrystallized. Highly fractured in most exposures. Forms cliffs. About 150 meters (490 ft) thick in the Pilot Range.

Ocw **Crystal Peak Dolomite and Watson Ranch Quartzite** (Ordovician) – Interlayered brown dolomite, gray silty limestone, brown sandy dolomite, and dolomitic quartzite. Forms gentle slopes. About 100 meters (330 ft) thick at Crater Island.

Ol **Lehman Formation** (Ordovician) – Thin-bedded, blue-gray, slightly silty, coarse-grained limestone with distinctive interbeds of ostracode and gastropod coquina. Contains sandy and silty beds and dark dolomite in uppermost part. Forms steep slopes. Lehman included within unit Ocw at Newfoundland Mountains. About 135 meters (440 ft) thick at Crater Island.

Ok **Kanosh Shale** (Ordovician) – Green and brown calcareous siltstone and gray-brown silty limestone. Forms slopes. About 140 meters (460 ft) thick in the Newfoundland Mountains. Queried where small outcrops preclude definite identification.

Opl **Lower Pogonip Group** (Ordovician) – Upper part is massive light- to medium-gray, slightly silty limestone forming steep slopes. Locally cherty. Lower part is thinly interbedded blue-gray limestone, gray and brown silty limestone, and brown calcareous siltstone. Forms prominent cliffs. About 470 meters (1540 ft) thick in the Newfoundland Mountains.

O€n **Notch Peak Formation** (Ordovician and Cambrian) – Dark-gray to black, medium- to thick-bedded dolomite and limestone. Upper part contains abundant, commonly black, chert nodules. Forms cliffs and steep slopes. About 500 meters (1640 ft) thick at Crater Island. In the Newfoundland Mountains, thick upper dolomite unit of Allmendinger and Jordan (1989) is provisionally assigned to the Notch Peak.

€cs **Corset Spring Shale Member of the Orr Formation** (Cambrian) – Brown, laminated to thin-bedded, calcareous siltstone and silty limestone. Forms saddles and gentle slopes. About 15 to 20 meters (50–66 ft) thick at Crater Island.

€j **Johns Wash Limestone Member of the Orr Formation** (Cambrian) – Medium- to thick-bedded limestone and dolomite forming tripartite section: upper part is white to gray, recrystallized marble; middle part is brownish-gray dolomite; lower part is dark-gray, slightly silty limestone. Forms steep slopes. About 80 to 120 meters (260–390 ft) thick at Crater Island.

€c **Candland Shale Member of the Orr Formation** (Cambrian) – Medium- to dark-gray, calcareous shale to silty limestone. Includes beds of red, calcareous, quartz sandstone and sandy limestone. Forms benches. About 60 meters (200 ft) thick at Crater Island.

€sd **Sandstone and dolomite** (Cambrian) – Thin- to medium-bedded dolomite to calcareous quartz sandstone. Greater than 125 meters (410 ft) thick in northern Newfoundland Mountains (Allmendinger and Jordan, 1989). Probably corresponds to the combined Corset Spring, Johns Wash, and Candland members of the Orr Formation.

€b **Big Horse Limestone Member of the Orr Formation** (Cambrian) – Dark-gray, thin-bedded, silty, oolitic limestone. Lower part is well-layered and silty; upper part is medium bedded to massive. Forms cliffs and steep slopes. About 180 meters (590 ft) thick at Crater Island. In the Newfoundland Mountains, middle dolomite unit and limestone unit of Allmendinger and Jordan (1989) are assigned to the Big Horse.

€l **Lamb Dolomite** (Cambrian) – Buff to light-gray, thick-bedded dolomite. Forms ledgey moderately steep slopes. About 75 meters (250 ft) thick at Crater Island. In the Newfoundland Mountains, lower dolomite unit of Allmendinger and Jordan (1989) is provisionally assigned to the Lamb; greater than 160 meters (535 ft) thick. Queried where small outcrops preclude definite identification.

€tr **Trippe Limestone** (Cambrian) – Black to dark-gray, thin-bedded, silty and oolitic limestone. Forms steep slopes. Greater than 135 meters (440 ft) thick at Crater Island.

€to **Toano Limestone** (Cambrian) – Gray to tan, platy, laminated and thin-bedded limestone and phyllitic limestone with dolomite and siltstone partings. Lower part is dark gray and grades into the underlying Killian Springs Formation. Structurally thinned (600 m [1960 ft] and less) in the Pilot Range, but about 850 meters (2800 ft) thick in the Toano Range, about 15 kilometers (10 mi) west of the Pilot Range (McCollum and Miller, 1991).

Ꞓks **Killian Springs Formation** (Cambrian) – Dark-colored, graphitic phyllite forming slopes. Lower part is homogeneous, dark-gray, black, and dark-blue-gray graphitic phyllite, and upper part is dark-gray calcareous phyllite. About 100 to 300 meters (330–990 ft) thick in the Pilot Range (McCollum and Miller, 1991).

ꞒZpm **Prospect Mountain Quartzite** (Cambrian and Neoproterozoic) – Light-colored, prominently bedded and cross-bedded quartzite forming massive cliffs. About 955 meters (3130 ft) thick where unit is complete in the central Pilot Range (Miller, 1983). Queried where small or weathered outcrops preclude definite identification.

McCoy Creek Group of Misch and Hazzard (1962) (Neoproterozoic) – Divided into:

Zmg **Unit G** – Dark phyllite and metasiltstone with interbedded marble and quartzite. Upper part consists of brown phyllite and less common quartzose conglomerate that thickens northward (Miller, 1983). Forms slopes. Thickens northward from about 480 to 1150 meters (1575–3775 ft).

Zmf **Unit F** – Thick-bedded, gray quartzite forming cliffs and steep slopes. Contains conglomerate lenses near top that include phyllite rip-up clasts. About 430 meters (1410 ft) thick. Queried where small outcrops preclude definite identification.

Zme **Unit E** – Brown laminated phyllitic argillite and metasiltstone. About 250 meters (820 ft) thick.

Zmd **Unit D** – Bedded to massive, poorly sorted gray to tan, conglomeratic quartzite forming cliffs. Generally feldspathic. About 220 meters (720 ft) thick.

Zmb **Unit B(?)** – White and gray, massive to laminated marble forming steep slopes. Provisionally assigned to Unit B by lithology; stratigraphic continuity with overlying McCoy Creek Group is uncertain. Greater than 155 meters (510 ft) thick.

Zma **Unit A(?)** – Interbedded tan flaggy quartzite, mica schist, and brown phyllite; upper part (about 60 to 80 m [200–260 ft] thick) contains light-green amphibole schist and minor brown mica schist. Provisionally assigned to Unit A by lithology; stratigraphic continuity with overlying McCoy Creek Group is uncertain. Forms slopes; greater than 450 meters (1475 ft) thick.

Triassic and Paleozoic rocks of Bovine Mountain, Terrace Mountain, and the Hogup and Grassy Mountains

Ŧd **Dinwoody Formation** (Triassic) – Yellow, reddish-gray, and brown, thin- to medium-bedded, impure limestone, calcareous shale, and siltstone. Typically fossiliferous. Forms slopes. Greater than 400 meters (1300 ft) thick at Terrace Mountain and about 600 meters (2000 ft) thick in the Hogup Mountains. Includes thin wedge of overlying siltstone of the Thaynes Formation (Triassic) in one place in the Hogup Mountains (Stifel, 1964).

Pg **Gerster Formation** (Permian) – Gray, shelly limestone, described previously. About 485 meters (1600 ft) thick at Terrace Mountain, about 600 meters (1970 ft) thick in the Hogup Mountains.

Pm **Murdock Mountain Formation** (Permian) – Dark-colored chert, sandstone, dolomite, and siltstone, described previously. About 1000 meters (3300 ft) thick at Terrace Mountain.

Ppm **Phosphoria Formation, Meade Peak Phosphatic Shale Tongue** (Permian) – Dark phosphatic shale, described previously. About 40 to 120 meters (130–400 ft) thick at Terrace Mountain, 200 meters (660 ft) thick at the Hogup Mountains.

Pgr **Grandeur Formation of the Park City Group** (Permian) – Sandy dolomite and dolomitic sandstone, described previously. About 560 meters (1840 ft) thick in the Hogup Mountains, where unit undergoes lateral change with decreasing chert. Chert-poor part was mapped as the Loray? Formation by Stifel (1964).

Pu **Unnamed sandstone unit** (Permian) – Light- to dark-gray, medium- to well-sorted medium- to thick-bedded sandstone, minor siltstone, limestone, and calcareous sandstone. Includes Diamond Creek Sandstone and part of a sandstone unit termed the Loray? Formation by Stifel (1964). Forms ledges. About 1630 meters (5350 ft) thick in the Hogup Mountains.

Oquirrh Group (Permian and Pennsylvanian) – Divided into:

Posl **Interbedded sandstone and limestone unit** (Permian) – Interbedded sandstone, siltstone, and subordinate silty limestone with chert. Chert more common in Hogup Mountains. About 1700 meters (5580 ft) thick at Bovine Mountains.

IPos **Sandstone unit** (Pennsylvanian) – Gray arkosic sandstone with interbeds of yellow siltstone, calcareous siltstone, sandy brown limestone, and bioclastic limestone; locally cherty. Minor quartzite and conglomerate. Forms ledge and bench topography. About 700 meters (2300 ft) thick at Bovine Mountain.

IPol **Limestone unit** (Pennsylvanian) – Gray, thick-bedded limestone with abundant chert. Thin interbeds of siltstone and sandstone, generally calcareous. Conglomerate beds locally. Forms prominent cliffs. About 500 meters (1650 ft) thick at Bovine Mountain.

Structurally thinned Pennsylvanian to Ordovician strata at Bovine Mountains (lithology of units conforms to units described in the previous section on the southern Pilot Range but some strata are missing):

IPMdc **Diamond Peak Formation and Chainman Shale, undivided** (Pennsylvanian and Mississippian)

Sl **Laketown Dolomite** (Silurian)

Oes **Ely Springs Dolomite** (Ordovician)

Oe **Eureka Quartzite** (Ordovician)

Ocw **Crystal Peak Dolomite and Watson Ranch Quartzite** (Ordovician)

Opl **Lower Pogonip Group** (Ordovician)

ACKNOWLEDGMENTS

We are grateful for the substantial mapping contributions by many who laid the groundwork before our studies began. Field visits by Lehi Hintze, Hellmut Doelling, Max Crittenden, Bob Compton, Rick Allmendinger, Terry Jordan, Susan Miller, and Don Fiesinger stand out among many others who helped us to understand the intricacies of the rock units in the area. Jack Oviatt's patient and frequent visits greatly increased our understanding of the Quaternary map units. Many co-workers contributed data and insights, including Anita Harris, Linda McCollum, Mike McCollum, Peter Sheehan, Bruce Wardlaw, Wendy Hillhouse, and John Nakata. A long list of talented field assistants and coauthors is associated with the many quadrangle geologic maps published in the area; among them, Lindee Berg, Andy Lush, Paddy McCarthy, and Joel Schneyer stand out. Padhrig T. McCarthy conducted field work for this map and did much of the initial digital map preparation, and Anne Elston also assisted with digital preparation. Reviews of the map by Joe Colgan and Dave John (USGS), and Jon King, Grant Willis, and Don Clark (UGS) improved earlier drafts and are greatly appreciated. Rosemary Fasselin (UGS) completed the GIS and cartography. This geologic map was funded by the U.S. Geological Survey, National Cooperative Geologic Mapping Program through FEDMAP funding.

REFERENCES

Allmendinger, R.W., and Jordan, T.E., 1984, Mesozoic structure of the Newfoundland Mountains, Utah—Horizontal shortening and subsequent extension in the hinterland of the Sevier belt: Geological Society of America Bulletin, v. 95, p. 1280–1292.

Allmendinger, R.W., and Jordan, T.E., 1989, Geologic map of the Newfoundland Mountains, Utah: U.S. Geological Survey Miscellaneous Field Investigations Map MF-2087, 1 sheet, scale 1:31,680.

Armstrong, R.L., 1970, Geochronology of Tertiary igneous rocks, eastern Basin and Range Province, western Utah, eastern Nevada, and vicinity, U.S.A.: Geochimica et Cosmochimica Acta, v. 34, p. 203–232.

Baranov, V.I., 1957, A new method for interpretation of aeromagnetic maps—Pseudo-gravimetric anomalies: Geophysics, v. 22, p. 359–383.

Baskin, R.L., and Turner, J., 2006, Bathymetric map of the north part of Great Salt Lake, Utah: U.S. Geological Survey Scientific Investigations Map 2954.

Best, M.G., Christiansen, E.H., Deino, A.L., Gromme, C.S., McKee, E.H., Noble, D.C., 1989, Eocene through Miocene volcanism in the Great Basin of the western United States: New Mexico Bureau of Mines and Mineral Resources Memoir 47, p. 91–133.

Blakely, R.J., 1995, Potential Theory in Gravity and Magnetic Applications: Cambridge University Press, Cambridge, England, 441 p.

Blakely, R.J., and Simpson, R.W., 1986, Approximating edges of source bodies from magnetic or gravity anomalies: Geophysics, v. 51, p. 1494–1498.

Cande, S.C., and Kent, D.V., 1995, Revised calibration of the geomagnetic polarity timescale for the late Cretaceous and Cenozoic: Journal of Geophysical Research, v. 100, p. 6093–6095.

Carroon, H.F., 1977, Petrochemistry and petrography of the Newfoundland stock, northwestern Utah: Stanford, California, Stanford University, Ph.D. dissertation, 241 p.

Chen, C.Y., and Maloof, A.C., 2017, Revisiting the deformed shoreline of Lake Bonneville: Quaternary Science Reviews, v. 159, p. 169–189.

Compton, R.R., 1983, Displaced Miocene rocks on the west flank of the Raft River-Grouse Creek core complex, Utah,

in Miller, D.M., Todd, V.R., and Howard, K.A., editors., Tectonic and stratigraphic studies in the eastern Great Basin: Geological Society of America Memoir 157, p. 271–279.

Compton, R.R., Todd, V.R., Zartman, R.E., and Naeser, C.W., 1977, Oligocene and Miocene metamorphism, folding, and low-angle faulting in northwestern Utah: Geological Society of America Bulletin, v. 88, p. 1237–1250.

Cook, K.L., Halverson, M.O., Stepp, J.C., and Berg, J.W., Jr., 1964, Regional gravity survey of the northern Great Salt Lake Desert and adjacent areas in Utah, Nevada, and Idaho: Geological Society of America Bulletin, v. 75, p. 715–740.

Cook, K.L., Bankey, Viki, Mabey, D.R., and DePangher, Michael, 1989, Complete Bouguer gravity anomaly map of Utah: Utah Geological and Mineral Survey Map 122, scale 1:500,000, https://doi.org/10.34191/M-122.

Cordell, L., and Grauch, V.J.S., 1985, Mapping basement magnetization zones from aeromagnetic data in the San Juan Basin, New Mexico, *in* Hinze, W.J., editor, The utility of regional gravity and magnetic anomaly maps: Society of Exploration Geophysicists, Tulsa OK, p. 181–192.

Crittenden, M.D., Jr., 1963, New data on the isostatic deformation of Lake Bonneville: U.S. Geological Survey Professional Paper 454-E, p. E1–E31.

Doelling, H.H., 1964, Geology of the northern Lakeside Mountains and the Grassy Mountains and vicinity, Tooele and Box Elder Counties, Utah: Salt Lake City, University of Utah, Ph.D. dissertation, 354 p., 5 sheets, scale 1:31,680.

Doelling, H.H., 1980, Geology and mineral resources of Box Elder County, Utah: Utah Geological and Mineral Survey Bulletin 115, 251 p., 3 sheets, scale 1:125,000, https://doi.org/10.34191/B-115.

Douglas, I.H., 1984, Geology and gold–silver mineralization of the Tecoma district, Elko County Nevada, and Box Elder County, Utah: Stanford, California, Stanford University, M.S. thesis, 135 p.

Egger, A.E., Dumitru, T.A., Miller, E.L., Savage, C.F.I., and Wooden, J.L., 2003, Timing and nature of Tertiary plutonism and extension in the Grouse Creek Mountains, Utah: International Geology Review, v. 45, p. 497–532.

Faulds, J.E., and Varga, R.J., 1998, The role of accommodation zones and transfer zones in the regional segmentation of extended terranes, *in* Faulds, J.E., and Stewart, J.H., editors, Accommodation zones and transfer zones—the regional segmentation of the Basin and Range Province: Geological Society of America Special Paper 323, p. 1–45.

Fiesinger, D.W., Greenman, E.R., Hare, E.M., Smith, K.W., and Voit, R.L., 1982, Chemistry and mineralogy of Tertiary(?) volcanic rocks from the eastern Great Basin, northwest Utah [abs]: Geological Society of America Abstracts with Programs, v. 15, p. 402–403.

Glick, L.L., and Miller, D.M., 1986, Geologic map of the Lucin 4 NW quadrangle, Box Elder County, Utah: Utah Geological and Mineral Survey Map 93, 4 p., 2 plates, scale 1:24,000, https://doi.org/10.34191/M-93.

Glick, L.L., and Miller, D.M., 1987, Geologic map of the Pigeon Mountain quadrangle, Box Elder County, Utah: Utah Geological and Mineral Survey Map 94, 9 p., 2 plates, scale 1:24,000, https://doi.org/10.34191/M-94.

Godsey, H.S., Currey, D.R., and Chan, M.A., 2005, New evidence for an extended occupation of the Provo shoreline and implications for regional climate change, Pleistocene Lake Bonneville, Utah, USA: Quaternary Research, v. 63, p. 212–223.

Grauch, V.J.S., and Cordell, L., 1987, Limitations of determining density or magnetic boundaries from the horizontal gradient of gravity or pseudogravity data: Geophysics, v. 52, no. 1, p. 118–121.

Heylmun, E.B., 1965, Reconnaissance of the Tertiary sedimentary rocks in western Utah: Utah Geological and Mineralogical Survey Bulletin 75, 38 p., https://doi.org/10.34191/B-75.

Jachens, R.C., and Moring, B.C., 1990, Maps of the thickness of Cenozoic deposits and the isostatic residual gravity over basement for Nevada: U.S. Geological Survey Open-File Report 90-404, 15 p., 2 plates.

Jordan, T.E., 1983, Structural geometry and sequence, Bovine Mountain, northwestern Utah, *in* Miller, D.M., Todd, V.R., and Howard, K.A., editors, Structural and stratigraphic studies in the eastern Great Basin: Geological Society of America Memoir 157, p. 215–227.

Khattab, M.M.M., 1969, Gravity and magnetic surveys of the Grouse Creek Mountains and the Raft River Mountains area and vicinity, Utah and Idaho: Salt Lake City, University of Utah, Ph.D. dissertation, 196 p.

Kim, K.Y., 1985, Seismic studies near Crater Island in the Great Salt Lake Desert, Utah: Norman, University of Oklahoma, M.S. thesis, 73 p.

Konstantinou, A., Strickland, A., Miller, E. L., Vervoort, J., Fisher, C. M., Wooden, J. P., and Valley, J., 2013, Syn-extensional magmatism leading to crustal flow in the Albion-Raft River-Grouse Creek metamorphic core complex northeastern Basin and Range: Tectonics, v. 32, p. 1384–1403.

Langenheim, V.E., 2016, Aeromagnetic map of northwest Utah and adjacent parts of Nevada and Idaho: Utah Geological Survey Miscellaneous Publication 16-4, 8 p., 1 plate, scale 1:250,000, https://doi.org/10.34191/MP-16-4.

Langenheim, V.E., Athens, N.D., Chuchel, B.A., Willis, H., Knepprath, N.E., Rosario, J., Roza, J., Kraushaar, S.M., and Hardwick, C.L., 2013, Preliminary isostatic gravity map of the Newfoundland Mountains and east part of the Wells 30' x 60' quadrangles, Box Elder County, Utah:

Utah Geological Survey Miscellaneous Publication 13-4, 3 p., 1 plate, 3 data files, scale 1:100,000, https://doi.org/10.34191/MP-13-4.

Lowry, A.R., and Perez-Gussinye, M., 2011, The role of crustal quartz in controlling Cordilleran deformation: Nature, v. 471, p. 353–357.

McCarthy, P.T., and Miller, D.M., 2002, Geologic map of the Terrace Mountain East quadrangle, Box Elder County, Utah: Utah Geological Survey Miscellaneous Publication 02-2, 14 p., 2 plates, scale 1:24,000, https://doi.org/10.34191/MP-02-2.

McCollum, L.B., and Miller, D.M., 1991, Cambrian stratigraphy of the Wendover area, Utah and Nevada: U.S. Geological Survey Bulletin 1948, 43 p.

McNeil, B.R., and Smith, R.B., 1992, Upper crustal structure of the northern Wasatch front, Utah, from seismic reflection and gravity data: Utah Geological Survey Contract Report 92-7, 76 p., https://doi.org/10.34191/CR-92-7.

Miller, D.M., 1983, Allochthonous quartzite sequence in the Albion Mountains, Idaho, and proposed Proterozoic Z and Cambrian correlatives in the Pilot Range, Utah and Nevada, *in* Miller, D.M., Todd, V.R., and Howard, K.A., editors, Tectonic and stratigraphic studies in the eastern Great Basin: Geological Society of America Memoir 157, p. 191–213.

Miller, D.M., 1985, Geologic map of the Lucin Quadrangle, Box Elder County, Utah: Utah Geological and Mineral Survey Map 78, 10 p., 2 plates, scale 1:24,000, https://doi.org/10.34191/M-78.

Miller, D.M., 1990a, Geologic map of the Lucin 4 SW quadrangle, Box Elder County, Utah: Utah Geological and Mineral Survey Map 130, 13 p., 2 plates, scale 1:24,000, https://doi.org/10.34191/M-130.

Miller, D.M., 1990b, Mesozoic and Cenozoic tectonic history of the northeastern Great Basin, *in* Shaddrick, D.R., Kizis, J.A., Jr., and Hunsaker, E.L., III, editors, Geology and ore deposits of the northeastern Great Basin: Geological Society of Nevada, p. 43–73.

Miller, D.M., 1990c, Geologic map of the Crater Island SW quadrangle, Box Elder County, Utah: Utah Geological and Mineral Survey Map 129, 8 p., 2 plates, scale 1:24,000, https://doi.org/10.34191/M-129.

Miller, D.M., 1993, Geologic map of the Crater Island NW quadrangle, Box Elder County, Utah: Utah Geological and Mineral Survey Map 145, 13 p., 2 plates, scale 1:24,000, https://doi.org/10.34191/M-145.

Miller, D.M., and Allmendinger, R.W., 1991, Jurassic normal and strike-slip faults at Crater Island, northwestern Utah: Geological Society of America Bulletin, v. 103, p. 1239–1251.

Miller, D.M., Clark, D.L., Wells, M.L., Oviatt, C.G., Felger, T.J., and Todd, V.R., 2012, Progress report geologic map of the Grouse Creek 30' x 60' quadrangle and Utah part of the Jackpot 30' x 60' quadrangle, Box Elder County, Utah, and Cassia County, Idaho (year 3 of 4): Utah Geological Survey Open File Report 598, 31 p., 1 plate, scale 1:62,500, https://doi.org/10.34191/OFR-598.

Miller, D.M., and Glick, L.L., 1986, Geologic map of the Lemay Island Quadrangle, Box Elder County, Utah: Utah Geological and Mineral Survey Map 96, 9 p., 2 plates, scale 1:24,000, https://doi.org/10.34191/M-96.

Miller, D.M., and Glick, L.L., 1987, Geologic map of the Jackson quadrangle, Box Elder County, Utah: Utah Geological and Mineral Survey Map 95, 7 p., 2 plates, scale 1:24,000, https://doi.org/10.34191/M-95.

Miller, D.M., Hillhouse, W.C., Zartman, R.E., and Lanphere, M.A., 1987, Geochronology of intrusive and metamorphic rocks in the Pilot Range, Utah and Nevada, and comparison with regional patterns: Geological Society of America Bulletin, v. 99, p. 866–879.

Miller, D.M., and Hoisch, T.D., 1995, Jurassic tectonics of northeastern Nevada and northwestern Utah from the perspective of barometric studies, *in* Miller, D.M., and Busby, C., editors, Jurassic magmatism and tectonics of the North American Cordillera: Geological Society of America Special Paper 299, p. 267–294.

Miller, D.M., Jordan, T.E., and Allmendinger, R.W., 1990a, Geologic map of the Crater Island quadrangle, Box Elder County, Utah: Utah Geological and Mineral Survey Map 128, 16 p., 2 plates, scale 1:24,000, https://doi.org/10.34191/M-128.

Miller, D.M., and Lush, A.P., 1994, Geologic map of the Pilot Peak quadrangle, Box Elder County, Utah, and Elko County, Nevada: Utah Geological Survey, Map 160, 25 p., 2 plates, scale 1:24,000, https://doi.org/10.34191/M-160.

Miller, D.M., Lush, A.P., and Schneyer, J.D., 1993, Geologic map of the Patterson Pass quadrangle, Box Elder County, Utah, and Elko County, Nevada: Utah Geological and Mineral Survey Map 144, 20 p., 2 plates, scale 1:24,000, https://doi.org/10.34191/M-144.

Miller D.M., and McCarthy, P.T., 2002, Geologic map of the Terrace Mountain West quadrangle, Box Elder County, Utah: Utah Geological Survey Miscellaneous Publication 02-3, 13 p., 2 plates, scale 1:24,000, https://doi.org/10.34191/MP-02-3.

Miller, D.M., Nakata, J.K., and Glick, L.L., 1990b, K-Ar ages for Jurassic to Tertiary plutonic and metamorphic rocks, northwestern Utah and northeastern Nevada: U.S. Geological Survey Bulletin 1906, 18 p.

Miller, D.M., Nakata, J.K., Oviatt, C.G., Nash, W.P., and Fiesinger, D.W., 1995, Pliocene and Quaternary volcanism in the northern Great Salt Lake area and inferred volcanic hazards, *in* Lund, W.R., editor, Environmental and Engineering geology of the Wasatch Front Region: Utah Geological Association Publication 24, p. 469–482.

Miller, D.M., and Oviatt, C.G., 1994, Geologic map of the Lucin NW quadrangle, Box Elder County, Utah: Utah Geological Survey Map 158, 14 p., 2 plates, scale 1:24,000, https://doi.org/10.34191/M-158.

Miller, D.M., Oviatt, C.G., and McGeehin, J.P., 2013, Stratigraphy and chronology of Provo shoreline deposits and lake-level implications, Late Pleistocene Lake Bonneville, eastern Great Basin, USA: Boreas, v. 42, p. 342–361.

Miller, D.M., and Phelps, G.A., 2016, The Pilot Valley shoreline, an early record of Lake Bonneville dynamics, in Oviatt, C.G., Shroder Jr., J.F., editors, Lake Bonneville—A Scientific Update: Developments in Earth Science Processes, v. 20, Elsevier, p. 60–74.

Miller, D.M., Repetski, J.E., and Harris, A.G., 1991, East-trending Paleozoic continental margin near Wendover, Utah, in Cooper, J.D., and Stevens, C.H., editors, Paleozoic paleogeography of the western United States–II: Pacific Section, Society of Economic Paleontologists and Mineralogists, v. 67, p. 439–461.

Miller, D.M., and Schneyer, J.D., 1985, Geologic map of the Tecoma Quadrangle, Box Elder County, Utah, and Elko County, Nevada: Utah Geological and Mineral Survey Map 77, 8 p., 2 plates, scale 1:24,000, https://doi.org/10.34191/M-77.

Miller, S.T., Martindale, S.G., and Fedewa, W.T., 1984, Permian stratigraphy of the Leach Mountains, Elko County, Nevada, *in* Kerns, G.J., and Kerns, R.L., Jr., editors, Geology of northwest Utah, southern Idaho and northeast Nevada: Utah Geological Association Publication 13, p. 65–78.

Misch, P., and Hazzard, J.C., 1962, Stratigraphy and metamorphism of late Precambrian rocks in central northeastern Nevada and adjacent Utah: American Association of Petroleum Geologists Bulletin, v. 46, p. 289–343.

Nelson, S.T., and Rey, K.A., 2018, Multi-proxy reassessment of the paleolimnology of Lake Bonneville (western USA) as observed in the restricted Pilot Valley sub-basin: Journal of Quaternary Science, v. 33, p. 177–193.

Oviatt, C.G., 2015, Chronology of Lake Bonneville, 30,000 to 10,000 yr B.P.: Quaternary Science Reviews, v. 110, p. 166–171.

Oviatt, C.G., Currey, D.R., and Miller, D.M., 1990, Age and paleoclimatic significance of the Stansbury shoreline of Lake Bonneville, eastern Great Basin: Palaeogeography, Palaeoclimatology, Palaeoecology, v. 99, p. 225–241.

Oviatt C.G., Currey, D.R., and Sack, D., 1992, Radiocarbon chronology of Lake Bonneville, northeastern Great Basin: Quaternary Research, v. 33, p. 291–305.

Oviatt, C.G., Miller, D.M., McGeehin, J.P., Zachary, C., and Mahan, S., 2005, The Younger Dryas phase of Great Salt Lake, Utah, USA: Palaeogeography, Palaeoclimatology, Palaeoecology, v. 219, p. 263–284.

Reimer, P.J., Bard, E., Bayliss, A., Beck, J.W., Blackwell, P.G., Ramsey, C.B., Buck, C.E., Cheng, H., Edwards, R.L., Friedrich, M., Grootes, P.M., Guilderson, T.P., Haflidason,H., Hajdas, I., Hatter, C., Heaton, T.J.,Hoffmann,D.L., Hogg, A.G., Hughen, K.A., Kaiser, K.F., Kromer, B., Manning, S.W., Niu, M., Reimer, R.W., Richards, D.A., Scott, E.M., Southon, J.R., Staff, R.A., Turney, C.S.M., van der Plicht, J., 2013, INTCAL13 and MARINE13 radiocarbon age calibration curves, 0–50,000 years cal BP: Radiocarbon, v. 55, p. 1869–1887.

Scarbrough, B.E., 1984, Structure and petrology of Tertiary volcanic rocks in parts of Toms Cabin Spring and Lucin NW quadrangles, Box Elder County, Utah: Logan, Utah State University, M.S. thesis, 77 p., scale 1:12,000.

Steele, G., 1960, Pennsylvanian-Permian stratigraphy of east-central Nevada and adjacent Utah: Intermountain Association of Petroleum Geologists 11th Annual Field Conference Guidebook, p. 91–113.

Stifel, P.B., 1964, Geology of the Terrace and Hogup Mountains, Box Elder County, Utah: Salt Lake City, University of Utah, Ph.D. dissertation, 173 p., scale 1:63,360.

Todd, V.R., 1983, Late Miocene displacement of pre-Tertiary and Tertiary rocks in the Matlin Mountains, northwestern Utah, *in* Miller, D.M., Todd, V.R., and Howard, K.A., editors, Tectonic and stratigraphic studies in the eastern Great Basin: Geological Society of America Memoir 157, p. 239–270.

Utah Division of Oil, Gas and Mining database (UDOGM): Online, https://oilgas.ogm.utah.gov/oilgasweb, accessed September 5, 2017.

Utah Division of Water Rights database (UDWR): Online, https://waterrights.utah.gov/wellinfo/wellinfo.asp, accessed September 11, 2017.

Wardlaw, B.R., Collinson, J.W., and Maughan, E.K., 1979, The Murdock Mountain Formation—a new unit of the Permian Park City Group, *in* Wardlaw, B.R., editor, Studies of the Permian Phosphoria Formation and related rocks: U.S. Geological Survey Professional Paper 1163B, p. 5–7.

Zietz, I., Shuey, R., and Kirby, J.R., Jr., 1976, Aeromagnetic map of Utah: U.S. Geological Survey Geophysical Investigations Map GP-907, scale 1:1,000,000.